



3 1293 01712 9119

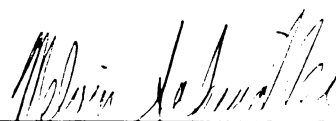
This is to certify that the
dissertation entitled
THE USE OF OPTICAL DISPLACEMENT MICROVISCOMETRY (ODM) AND
RECONSTITUTED MODEL SYSTEMS TO MEASURE ALUMINUM INDUCED
CHANGES IN THE ORGANIZATION AND VISCOSITY OF ACTIN

presented by

Eric J. Arnoys

has been accepted towards fulfillment
of the requirements for

Ph.D. degree in Biochemistry


Major professor

Date 12/19/97

LIBRARY
Michigan State
University

PLACE IN RETURN BOX
to remove this checkout from your record.
TO AVOID FINES return on or before date due.

DATE DUE	DATE DUE	DATE DUE

**THE USE OF OPTICAL DISPLACEMENT MICROVISCOMETRY (ODM) AND
RECONSTITUTED MODEL SYSTEMS TO MEASURE ALUMINUM INDUCED
CHANGES IN THE ORGANIZATION AND VISCOSITY OF ACTIN**

By

Eric J. Arnoys

A DISSERTATION

Submitted to
Michigan State University
in partial fulfillment of the requirements
for the degree of

DOCTOR OF PHILOSOPHY

Department of Biochemistry

1998

ABSTRACT

THE USE OF OPTICAL DISPLACEMENT MICROVISCOMETRY (ODM) AND RECONSTITUTED MODEL SYSTEMS TO MEASURE ALUMINUM INDUCED CHANGES IN THE ORGANIZATION AND VISCOSITY OF ACTIN

By

Eric J. Arnoys

Absorption of aluminum from acidic soils and surface waters can have significant adverse consequences for plant growth and development. Such deleterious effects range from stunted root growth to death. Despite the agricultural importance of the problem and years of intense study, investigations have yielded neither definitive targets nor unambiguous molecular mechanism(s) for aluminum toxicity in plant cells.

Recent findings in our laboratory suggest that aluminum may function as a cytoskeletal toxicant. Evidence has been presented that the actin filament network is a potential target for the adverse effects of aluminum in plant cells. Aluminum interaction with actin networks can modify the dynamic properties of these actin filaments sufficiently to result in the abnormal growth phenotypes observed for aluminum toxicity. This dissertation describes the development of a new assay, Optical Displacement Microviscometry (ODM), to measure the viscosity of actin solutions in a reconstituted model system. The experiments performed with this technique in a reconstituted system were designed to characterize the components of the actin network and their interactions that are potentially affected by the addition of aluminum. An attractive feature of the ODM technique is that it utilizes a laser optical trap to perform viscosity measurements in microvolumes of solution (~ 10 μ l) and only requires minute quantities of precious

sample. Confocal fluorescence microscopy was utilized in conjunction with the ODM technique to examine the organization of the actin network. Results obtained from both techniques were employed to correlate the organization of the filament networks within the actin solution to the viscosity of the reconstituted system.

In pure actin solutions, the effects of aluminum were not apparent until after the addition of nonphysiologically high concentrations. However, inclusion of an actin binding protein that cross-links actin filaments, e.g., myosin or filamin, altered the organization of the actin solution in a way that decreased the concentration of aluminum (20 μM) that was required to cause dramatic effects on the measured viscosity. The changes in the viscosity of actin/myosin solutions induced by aluminum were observed regardless of the type of actin (rabbit muscle, human platelet, or maize pollen) examined in the model system. The changes in viscosity observed with aluminum could also be seen with confocal fluorescence microscopy as changes in the organization and interaction of actin filaments. The data obtained using the reconstituted actin systems, the ODM, and confocal fluorescence microscopy provide support for a mechanism of aluminum toxicity in which physiologically relevant concentrations of aluminum can promote/enhance the interaction of actin filaments in the presence of actin crosslinking proteins, resulting in abnormal activity for actin dependent cellular activities.

Gloria Deo Soli

Acknowledgements

I would like to thank my mentor Dr. Melvin Schindler for his guidance during my years at Michigan State. In his laboratory I learned much about science, thought, and experimental design; but he also taught me a great deal about the values of a complete education, seeing things fully, and using common sense. After five years I think that I finally know the difference between “doing one’s best” and “doing what it takes.” I greatly appreciate having been treated like a peer, especially on those days when things weren’t working as well as anticipated. Thank you.

I would also like to thank Dr. John Wang, who played an integral role in my education. He and his lab group taught me much about the art of presentation. I am grateful for the combination of his encouragement, demands for excellence, and friendship during my study and pursuit of a career.

Thank you to the members of my guidance committee: Drs. Steve Heidemann, Ken Keegstra, Leslie Kuhn, and Jack Preiss. I would especially like to thank Leslie for her continuous encouragement and support as I sorted through a variety of technical challenges on this project.

I owe much gratitude to my friends and colleagues in the Schindler/Wang lab group for their help and for passing on the Lunch Bunch tradition: Sharon Grabski, Patty Voss, Dr. John Ho, Dr. John Loh, Dr. Anandita Vyankarnum, Dr. Sung-Yuan Wang, Mark Kadrofske, Dr. Yeou-Guang Tsay, Benjamin Busch, Jennifer Rutzen, Andy

Lenneman, Kyle Openo, and Nancy Lin. Thank you also to Matias Vicente Cruz and Miguel Proano for aiding me with my project. Special thanks to Patty, Mark, Kyle, and Sharon.

Thank you to those friends (too numerous to name) who have helped me out through the years. I would not have made it without you. At the top of my list are many from East Lansing—Lissa, Jeff, Al, Amy, Rob, Randy, Brian, Tim, Per, Heidi, Mike, Cathy, Shelly. Long live Delta 5—Dave, Tim, John, Jeff, Randy, Carol, Jany, and Laura. Thank you also to Tricia and John for the years of friendship.

Most of all, I appreciate the support (and patience) of my family. Marc, Rob, Dawn, and Travis—I love you guys. But thanks most of all to Mom and Dad.

Yes, Dad, I have started writing.

TABLE OF CONTENTS

LIST OF FIGURES	ix
LIST OF ABBREVIATIONS	xii
CHAPTER 1:	
LITERATURE REVIEW	1
INTRODUCTION	1
Cytotoxicity of Aluminum Ion	1
Actin	6
Architecture of Actin Filaments	7
REFERENCES	12
CHAPTER 2:	
OPTICAL DISPLACEMENT MICROVISCOMETRY (ODM) AND ACTIN	16
ABSTRACT	16
INTRODUCTION	17
MATERIALS AND METHODS	20
Preparation of F-actin from Rabbit Muscle	21
Acetone Powder	
Non-muscle and Plant Actin	21
Preparation of Muscle Actin for Viscometry	22
Capillary Viscometry	22
Optical Displacement Microviscometry (ODM)	23
Preparation of Microscope Slides for ODM	23
Visualization of Actin Filaments	23
SDS-PAGE Analysis	24
RESULTS	27
SDS-PAGE of Protein Samples	27
Optical Displacement Microviscometry	27
ODM of Actin Solutions	31
Bead Radius and Effective Drag	36
Effects of Cytochalasin D and Phalloidin	39
Non-muscle Actin	42
Plant Actin	42
Measurements of Actin Organization and Viscosity	47
DISCUSSION	51
REFERENCES	54

CHAPTER 3:	
ALUMINUM AND THE ACTIN NETWORK	56
ABSTRACT	56
INTRODUCTION	57
MATERIALS AND METHODS	60
Myosin ATPase Assays	61
RESULTS	65
Effect of Aluminum on Actin Polymerization and Structure	65
Al ³⁺ Effect is Ion Specific	68
Reversal of Aluminum Effect by NaF	75
Aluminum and ATP	76
The Actin-Binding Protein Myosin	81
Myosin—A Potential Regulator within the Actin Network	81
Addition of Aluminum to a Solution of Actin/Myosin	82
Non-muscle Actin with Myosin	87
Plant Actin with Myosin	87
Ion Specificity of Aluminum Effect	94
Heating of Myosin	94
Intact Actin Network is Necessary for the Al ³⁺ Effect	101
ATPase Assays	106
The Actin-bundling Protein Filamin	106
Aluminum and Actin/Filamin Complexes	111
DISCUSSION	116
REFERENCES	121
 CHAPTER 4:	
CONCLUDING STATEMENT	124

LIST OF FIGURES

CHAPTER 2

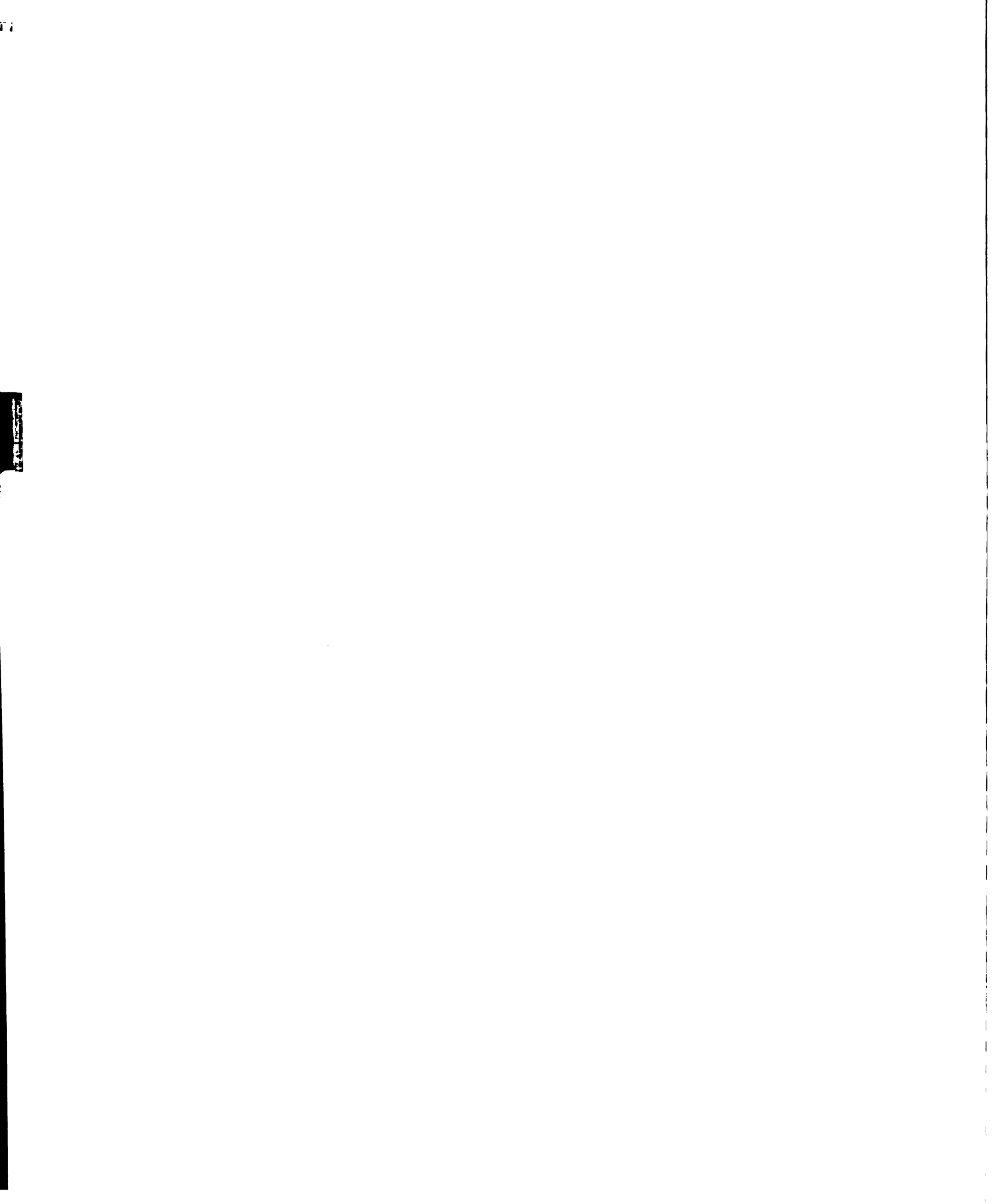
Figure 1. SDS-PAGE of actin samples	26
Figure 2. Optical trapping of polystyrene microspheres	29
Figure 3. Comparison of capillary viscometry with Optical Displacement Microviscometry (ODM).	33
Figure 4. ODM measurements performed on solutions of rabbit muscle F-actin.	35
Figure 5. An evaluation of the effective drag as a function of bead radius.	38
Figure 6. Effects of fungal alkaloids on the viscosity and organization of F-actin.	41
Figure 7. Measurements of the viscosity and organization of F-actin purified from human platelets.	44
Figure 8. Measurement of the viscosity and organization of F-actin purified from maize pollen.	46
Figure 9. The effect of gelsolin in the absence and presence of calcium on the viscosity and organization of rabbit muscle F-actin.	49

CHAPTER 3

Figure 1. SDS-PAGE of actin and actin binding proteins	64
Figure 2. Measurements of the viscosity and organization of rabbit muscle F-actin in the absence and presence of aluminum	67

Figure 3. The effect of aluminum on the viscosity and organization of human platelet actin.	70
Figure 4. The effect of aluminum on the viscosity and organization of maize pollen actin.	72
Figure 5. The specificity of aluminum in promoting changes in F-actin networks.	74
Figure 6. The reversal of the aluminum effect by incubation with NaF..	78
Figure 7. ODM measurements of F-actin solutions in the presence of excess ATP.	80
Figure 8. ODM measurements of solutions of rabbit muscle F-actin in the presence of myosin	84
Figure 9. Effect of aluminum on solutions of rabbit muscle F-actin/bovine muscle myosin II	86
Figure 10. ODM measurements of solutions of myosin/non-muscle F-actin.	89
Figure 11. Effect of aluminum on solutions of myosin/non-muscle actin.	91
Figure 12. ODM measurements of myosin/maize pollen actin solutions	93
Figure 13. Effect of aluminum on myosin/maize pollen actin solutions.	96
Figure 14. The effect of aluminum on myosin/actin complexes is specific	98
Figure 15. Reversal of aluminum-induced viscosity change by fluoride.	100
Figure 16. Heat treatment inhibits the effect of aluminum on the viscosity and organization of solutions of myosin/actin	103
Figure 17. Capillary viscometry of bovine muscle myosin II.	105
Figure 18. The effect of cytochalasin D and latrunculin on aluminum-induced changes in solutions of myosin/actin.	108

Figure 19. Assays of myosin ATPase activity.	110
Figure 20. ODM measurements of solutions of filamin/actin	113
Figure 21. Effect of aluminum on solutions of filamin/actin	115



LIST OF ABBREVIATIONS

ATP	adenosine triphosphate
β ME	2-mercaptoethanol
BSA	bovine serum albumin
C_c	critical concentration
DMSO	dimethyl sulfoxide
EDTA	ethylenediaminetetraacetic acid
F-actin	filamentous (polymerized) actin
FILC	Fluorescence Interactive Laser Cytometer
G-actin	globular (monomeric) actin
HPLC	high performance liquid chromatography
KDa	kilodaltons
ODA	Optical Displacement Assay
ODM	Optical Displacement Microviscometry
SDS-PAGE	sodium dodecylsulfate polyacrylamide gel electrophoresis

Chapter 1

INTRODUCTION

Cytotoxicity of aluminum ion.

Aluminum is the most abundant metal in the earth's crust, constituting approximately seven percent of the total mass (Macdonald and Martin, 1988; Delhaize and Ryan, 1992; Flaten, et al., 1996; Sparling and Lowe, 1996). Though nearly 40% of the arable soil in the world has high concentrations of aluminum (Flaten, et al., 1996), most of it remains insoluble at neutral pH in the form of aluminosilicates or hydroxides, trapped in clays, or chelated by organic acids and phosphates (Macdonald and Martin, 1988; Delhaize and Ryan, 1992; Sparling and Lowe, 1996). However, in regions of the world where industrial runoffs, leaching of soils, and acid rain have acidified soils and surface water, free aluminum ion can be found in the soil at appreciable concentrations. Increased aluminum solubility can lead to increased uptake of free aluminum by plants and animals.

High concentrations of aluminum have been shown to cause chronic renal failure, encephalopathy, osteomalacia, and dementia in long-term dialysis patients (Macdonald and Martin, 1988; Flaten, et al., 1996). Fish exposed to aluminum in acidified lakes suffer asphyxiation upon continued exposure of their gills to aluminum, as well as damage to the central nervous system reminiscent of that seen in some human neurodegenerative diseases (Driscoll, et al., 1980; Flaten, et al., 1996). Rats given

aluminum-treated drinking water were found to have measurable amounts of aluminum in brain tissue (Walton, et al., 1995). In humans, accumulation of aluminum in the brain has been associated with the neurofibrillary tangles and plaques observed to correlate with the development of Alzheimer's disease (Flaten, et al., 1996; Fasman, et al., 1995; Savory, et al., 1996). Whether these accumulations are causative, contributory or unrelated remains to be rigorously determined.

The physiological effects of aluminum on plant growth are more clear. Increased acidity of soils containing high concentrations of aluminum results in the inhibition of root growth and plant development (Ryan, et al., 1994; Delhaize and Ryan, 1995; Sparling and Lowe, 1996). Die-backs of forests in regions of acid rain have been attributed to increases in aluminum solubility and uptake (Sparling and Lowe, 1996). Pollen tube growth and extension is also inhibited by low concentrations of aluminum under acidic environmental conditions (Konishi and Miyamoto, 1983).

Though aluminum uptake is known to be responsible for a diverse array of physiological effects, the biochemical mechanism(s) of aluminum toxicity has yet to be elucidated (Macdonald and Martin, 1988; Delhaize and Ryan, 1995). However, the levels of toxicity for the various ionic species of aluminum have been determined. In neutral solutions, aluminum forms a precipitate of $\text{Al}(\text{OH})_3$ (Macdonald and Martin, 1988). As a solution of aluminum becomes more acidic, resulting in a shift of ionic species from $\text{Al}(\text{OH})_2^+$ to $\text{Al}(\text{H}_2\text{O})_6^{3+}$ (also denoted as free aluminum or Al^{3+}), the precipitate becomes more soluble. Free aluminum can form high affinity complexes with PO_4^{3-} , SO_4^{2-} , HCO_3^- , F^- , hydroxides, organic acids, proteins, and lipids (Delhaize and Ryan, 1995; Sparling and Lowe, 1996). Of the biologically important ions, Al^{3+} is

thought to be most comparable with Mg^{2+} , since their effective ionic radii most closely resemble each other (Macdonald and Martin, 1988). Although the two ions bear different charges, competition between them for binding to molecules appears to depend more on ionic radius than charge. Aluminum binds to nucleoside triphosphates $\sim 10^7$ times better than Mg^{2+} , and the slow rate of exchange of aluminum with the solution can interfere with the hydrolysis of the phosphate bonds (Macdonald, et al., 1987).

Several species of plants exhibit an aluminum resistance phenotype by regulating the synthesis of anionic molecules that can chelate free aluminum. Secreted or internally accumulated organic acids such as citrate, malate, and succinate have been shown to chelate aluminum *in vivo*, either by precipitating the aluminum outside the plant cell cytoplasm or by capturing and sequestering aluminum within the cytoplasm or vacuolar compartments (Delhaize, et al., 1993; Ma, et al., 1997). Overexpression of enzymes regulating citrate synthesis has also been shown to induce aluminum tolerance within non-tolerant strains of wheat (de la Fuente, et al., 1997).

Current hypotheses suggest a number of different potential mechanisms for aluminum toxicity. Since Al^{3+} can bind tightly to Mg^{2+} -coordination sites on nucleoside triphosphates, slowing the rate of hydrolysis considerably (Macdonald, et al., 1987), it has been suggested that aluminum may in this way interfere with energy-dependent enzymes (Grabski and Schindler, 1995). A recently published report suggests an alternate possibility. Physiologically-relevant aluminum concentrations were incubated with energy-dependent enzymes with catalytic metal binding sites to see if they would alter enzymatic activity (Jones and Kochian, 1997). Much to their surprise, investigators found that enolase, pyruvate kinase, H^+ -ATPase, Ca^{2+} -ATPase, Ca^{2+} -protease, myosin,

Proteinase K, and arginase were not affected by free aluminum. The only enzymes significantly altered were phospholipase A₂ (PLA₂) (Jones and Kochian, 1997) and phospholipase C (Jones and Kochian, 1995). The effects on PLA₂ may possibly be explained by interaction of Al³⁺ with phospholipids (Jones and Kochian, 1997), the substrate for PLA₂.

Aluminum has also been proposed to alter ion-transport channels, either through an allosteric mechanism or by interfering with transport of ions through the channels themselves. Detailed studies with Ca²⁺ have shown that aluminum neither alters intracellular Ca²⁺ transport (Ryan, et al., 1994), nor interferes with the sensing of calcium levels within the cell (Delhaize and Ryan, 1995). Indirect evidence also suggests that aluminum may influence callose synthesis in plants, a process which requires an increase in Ca²⁺ levels and can be stimulated by several polyvalent cations (Rengel, 1992). Additionally, aluminum can inhibit K⁺ uptake in root hairs (Gassman and Schroeder, 1994) and may also interfere with the transport of iron by transferrin (Macdonald and Martin, 1988).

Free aluminum can bind to calmodulin at sites distinct from Ca²⁺-binding sites. Stoichiometric levels of aluminum can induce conformational changes in calmodulin, altering its affinity for melittin, a probe which simulates the target enzymes of calmodulin (Weiss and Haug, 1987). Upon binding of aluminum, the conformation of calmodulin is changed such that the calmodulin target region looks more polar, perhaps interfering with its activity. Should calmodulin activity be altered by aluminum, a number of regulatory processes could be simultaneously affected within the cell.

Although most investigations have examined the influence of aluminum on either

soluble factors within the cell or components of the cell membrane, the cytoskeleton has also been proposed to be a target of aluminum toxicity. In patients with Alzheimer's disease, aluminum can be localized to neurofibrillary tangles, a characteristic feature of the illness. The microtubule-associated protein tau is a major component of these tangles; aggregation of tau can be induced within one day upon addition of micromolar concentrations of aluminum maltolate (Savory, et al., 1995).

Recent findings by our lab have provided further insight into possible mechanisms for aluminum toxicity in plants. Upon addition of micromolar concentrations of aluminum to a soybean (*Glycine Max* [L.] Merr. cv. Mandarin) cell suspension (originally derived from roots) in 1B5C medium (Metcalf, et al., 1983), the actin containing fibers within the transvacuolar strands of cells exhibit an increase in stiffness and a concomitant loss of elasticity (Grabski and Schindler, 1995). Aluminum-induced stiffness is prevented by pre-incubation of the cells with cytochalasin D, a fungal alkaloid which depolymerizes actin. Pollen tube growth and plant cell division are both highly dependent on the actin-based cytoskeleton; therefore any change in the viscoelastic properties of the actin network could result in alterations in growth, cell differentiation and development.

Further studies from our laboratory have provided additional support for the view that the actin network may be a principal target for aluminum mediated toxicity (Grabski, et al., 1998). Drugs which affect the myosin/actin network alter the cytoskeleton in a predictable fashion and can decrease or enhance the effect of free aluminum. Likewise, the *in vivo* addition of drugs that inhibit the activity of specific kinases and phosphatases, both potential regulatory components of the actin network, modifies the ability of

aluminum to influence the tension within the actin network.

These observations support a role for the actin filament network in aluminum toxicity in plant cells and suggest the importance of developing a model system comprised of purified actin and actin binding proteins to determine the molecular targets for aluminum activity within the actin network.

Actin

Actin is a globular protein of 42 KDa which can polymerize to form a filamentous network. Actin is found in relatively high concentrations in cells, where it is involved in many cellular functions, including muscle contraction (Pardee and Spudich, 1982), directed organelle locomotion and localization (Simon, et al., 1995), cellular motility (Lauffenburger and Horwitz, 1996; Mitchison and Cramer, 1996), postmitotic cell spreading (Cramer and Mitchison, 1995), cell shape and integrity (Pasternak and Ellson, 1985), cell polarity (Drubin and Nelson, 1996), and cytoplasmic streaming in plants (Kohno and Shimmen, 1988).

The amino acid sequence of actin has been highly conserved throughout evolution, both within and between species (Pollard and Cooper, 1986). Plants contain approximately 60 actin genes, suggesting tissue-specific expression of plant actin genes (McLean, et al., 1990). Comparison of actins between species reveals an 80% identity in amino acid residues between animals and plants (Hightower and Meagher, 1986). Such close identity supports the importance of actin function, as well as the likelihood that different types of actin will have similar physical behavior.

Monomeric, or globular, actin (G-actin) above a critical concentration (C_c) of 0.1

μM polymerizes to form filaments (F-actin) (Korn, et al., 1987). Polymerization requires adenine nucleoside and mono- and divalent cations (usually K^+ and Mg^{2+}). Though ADP will allow polymerization to occur, monomers with bound ATP associate more readily with actin filaments (Pollard, et al., 1992). These filaments are in a state of dynamic equilibrium; actin monomers can associate and dissociate from either end at any time unless the end is associated with a bound capping protein (Pollard and Cooper, 1986).

Actin monomers also have ATPase activity, though the physiological consequences of ATP hydrolysis are still a matter of conjecture (Korn, et al., 1987; Janmey, et al., 1990; Pollard, et al., 1992). Following polymerization, ATP is hydrolyzed, though the subsequent release of inorganic phosphate occurs slowly (Korn, et al., 1987). Although ATP hydrolysis can stabilize the filament upon formation of $\text{ADP}\cdot\text{P}_i$, it is not required for polymerization (Korn, et al., 1987). The identity of adenosine nucleoside bound to actin affects the critical concentration of a monomer, with ADP-actin having a C_c approximately eight times that of ATP-actin. Since filaments are polar, each end of a given filament can have a different C_c . When the concentration of monomer lies between these two values, monomers will add to one side of the filament and dissociate at the other (Pollard and Cooper, 1986) This phenomenon is known as “treadmilling.”

Architecture of actin filaments.

Actin filaments form a complex network within the cytoplasm of both plants and animal cells. They are flexible along their lengths and can turn along their longitudinal axes (Pollard and Cooper, 1986). The filaments demonstrate the physical property of

viscoelasticity (Buxbaum, et al., 1987; Zaner and Valberg, 1989) and are essential structural elements of the cell.

The demands of different cell shapes, locations, and functions require that actin be quite versatile. Some cells need a rapid synthesis of F-actin, whereas others rapidly reorganize the existing interacting networks. Actin provides stiffness and structure within the cytoplasm and along the plasma membrane of cells such as erythrocytes (Elson, 1988). A diverse population of actin-binding proteins permits cells to arrange actin into a multiplicity of structures with differing physical properties.

Some cellular events require rapid solution of the actin filament network. This can be accomplished with actin severing proteins, such as gelsolin and actophorin. Gelsolin binds to actin filaments and, in the presence of Ca^{2+} , severs them and caps the ends (Bearer, 1991). In a short time, gelsolin can transform a gel comprised of long, networked filaments into a solution of small F-actin pieces. Actophorin, an actin-severing protein found in *Acanthamoeba*, is controlled by inorganic phosphate rather than Ca^{2+} (Maciver, et al., 1991b). Actophorin can sever spontaneously-forming F-actin and, coupled with α -actinin, helps form stiff bundles of short, relatively uniformly-sized actin filaments (Maciver, et al., 1991a).

Another important group of actin-binding proteins are those which contain two actin-binding sites to crosslink filaments. The resulting filament structure depends largely upon the geometry of the cross-linker. Narrow spacing between actin-binding sites allows fimbrin and villin to give support to the plasma membrane in microvilli by crosslinking actin into tight bundles (Matsudaira, 1991). Spectrin, a large tetramer with widely-spaced actin-binding sites, forms networks in erythrocytes, giving them strength

and structure by linking the cytoskeleton to membranes or membrane-anchored proteins (Pollard and Cooper, 1986). Filamin, a crosslinker found in many cell types, is a homodimer which crosslinks overlapping filaments to form three-dimensional networks (Pollard and Cooper, 1996).

An actin-binding protein of particular importance for plant function is the molecular motor myosin, the only known crosslinker of actin filaments for which evidence has thus far been presented in plants (Knight and Kendrick-Jones, 1993; Kinkema and Schiefelbein, 1994). Though five isoforms of myosin have been characterized in animal cells and yeast (Cheney, et al., 1993), sequence comparisons indicate that the plant myosins characterized so far most resemble Type V myosin (Knight and Kendrick-Jones, 1993; Kinkema and Schiefelbein, 1994). Type V myosin can dimerize, allowing it to bind two actin filaments simultaneously

Much of what is known about actin and the proteins which interact with the monomeric or polymerized forms has been discovered through the use of *in vitro* systems. The viscosity of actin solutions changes with the polymerization state of actin. Cross-linking, bundling, and severing all influence the gel or solution state of actin (Janson, et al., 1991). Actin severing proteins such as actophorin reduce solution structure by severing actin filaments (Maciver, et al., 1991b). Monomer-binding proteins shift the concentration of free monomer, leading to dissociation and shortening of the filaments (Fechheimer and Zigmond, 1993). Structural changes induced by actin cross-linking proteins are determined by protein geometry and size. Bundling and crosslinking contribute to different types of filament organization and corresponding differences in filament behavior in solutions. Crosslinked networks form loose, viscous gels, whereas

thick bundles tend to be more rigid and form less fluid-like domains.

In vitro studies of the diffusion of inert tracer molecules in actin gels have provided a model for the submicroscopic architecture of actin in the cytoplasm (Hou, et al., 1990a; Hou, et al., 1990b). A suspension of long actin filaments could be distinguished from a crosslinked filament network at the microscopic level. Tangling of F-actin filaments created a matrix in which diffusion was dependent strictly upon particle size and F-actin concentration. Crosslinked samples contained regions of densely-packed filaments, as well as areas in which the void volume had become more accessible to particles. Based on these results, Hou et al. (1990b) proposed that the cytoplasm of the cell consists of two regions: a fluid phase filled with proteins and other macromolecules, and a gel phase composed of crosslinked actin filaments.

The complex behavior of these solutions and their structures can be examined by viscosity measurements. Dispersed networks of long filaments form gels with high viscosity. Shorter filaments, or those cross-linked into tight bundles, tend to have a lower viscosity. Much of what is known about solutions has been determined by viscosity measurements.

Study of actin and its filament structure has been aided tremendously by microscopy. Antibodies directed against actin or its binding proteins have been used to localize proteins *in vivo* and to examine solution structure *in vitro*. F-actin can be labeled specifically by phalloidin, a fungal cytotoxin which binds in the region between two subunits of the actin filament (Dancker, et al., 1975; Cooper, 1987). Fluorescent conjugates of phalloidin have allowed examination of filament structure by confocal fluorescence microscopy.

This dissertation describes the development and use of an *in vitro* assay to examine the viscosity of both plant and animal (muscle and non-muscle) F-actin filament networks in the absence and presence of aluminum. In addition, these measurements are also performed in the presence of actin binding proteins to determine if the changes in the viscosity are uniquely dependent on F-actin or require additional components to function as mediators. Consolidation of this information provides a mechanism which can be reconciled with the *in vivo* data to help explain the toxic effects of aluminum on the actin filament network.

REFERENCES

- Bearer EL (1991) Direct observation of actin filament severing by gelsolin and binding by gCap39 and CapZ. *J Cell Biol* **115**: 1629-38
- Buxbaum RE, Dennerll T, Weiss S, Heidemann SR (1987) F-actin and microtubule suspensions as indeterminate fluids. *Science* **235**: 1511-4
- Cheney RE, Riley MA, Mooseker MS (1993) Phylogenetic analysis of the myosin superfamily. *Cell Motil Cytoskeleton* **24**: 215-23
- Cooper JA (1987) Effects of cytochalasin and phalloidin on actin. *J Cell Biol* **105**: 1473-8
- Cramer LP, Mitcheson TJ (1995) Myosin is involved in postmitotic cell spreading. *J Cell Biol* **131**: 179-89
- Dancker P, Löw I, Hasselbach W, Wieland T (1977) Interaction of actin with phalloidin: polymerization and stabilization of F-actin. *Biochem Biophys Acta* **400**: 407-14
- de la Fuente JM, Ramírez-Rodríguez V, Cabrera-Ponce L, Herrera-Estrella L (1997) Aluminum tolerance in transgenic plants by alteration of citrate synthase. *Science* **276**: 1566-8
- Delhaize E, Ryan PR, Randall PJ (1993) Aluminum tolerance in wheat (*Triticum aestivum* L.). II. Aluminum-stimulated excretion of malic acid from root apices. *Plant Physiol* **103**: 695-702
- Delhaize E, Ryan PR (1992) Aluminum toxicity and tolerance in plants. *Plant Physiol* **107**: 315-21
- Driscoll CT Jr., Baker JP, Bisogni JJ Jr., Schofield CL (1980) Effect of aluminum speciation on fish in dilute acidified waters. *Nature* **284**: 161-4
- Drubin DG, Nelson WJ (1986) Origins of cell polarity. *Cell* **84**: 335-44
- Elson, EL (1988) Cellular mechanics as an indicator of cytoskeletal structure and function. *Ann Rev Biophys Biophys Chem* **17**: 397-430
- Fasman GD, Perczel A, Moore CD (1995) Solubilization of β -amyloid-(1-42)-peptide: reversing the β -sheet conformation induced by aluminum with silicates. *Proc Nat Acad Sci* **92**: 369-71
- Fechheimer M, Zigmond SH (1993) Focusing on unpolymerized actin. *J Cell Biol* **123**: 1-5

- Flaten TP, Alfrey AC, Birchall JD, Savory J, Yokel RA (1996) Status and future concerns of clinical and environmental aluminum toxicology. *J Tox Env Health* **48**: 527-41
- Gassmann W, Schroeder JI (1994) Inward-rectifying K⁺ channels in root hairs of wheat. *Plant Physiol* **105**: 1399-408
- Grabski S, Arnoys E, Busch BA, Schindler M (1998) Dynamic modification of tension within the actin network in plant cells by calcium regulated kinases and phosphatases. *Plant Physiol* **116**: 279-90
- Grabski S, Schindler M (1995) Aluminum induces rigor within the actin network of plant cells. *Plant Physiol* **108**: 897-901
- Griffith LM, Pollard TD (1982) Cross-linking of actin filament networks by self-association and actin-binding macromolecules. *J Biol Chem* **257**: 9135-42
- Hightower RC, Meagher RB (1986) The molecular evolution of actin. *Genetics* **114**: 315-32
- Hou L, Lanni F, Luby-Phelps K (1990a) Tracer diffusion in F-actin and ficoll mixtures. Toward a model for cytoplasm. *Biophys J* **58**: 31-43
- Hou L, Luby-Phelps K, Lanni F (1990b) Brownian motion of inert tracer macromolecules in polymerized and spontaneously bundled mixtures of actin and filamin. *J Cell Biol* **110**: 1645-54
- Janmey PA, Hvidt S, Oster GF, Lamb J, Stossel TP, Hartwig JH (1990) Effect of ATP on actin filament stiffness. *Nature* **347**: 95-9
- Janson LW, Kolega J, Taylor DL (1991) Modulation of contraction by gelation/solution in a reconstituted motile model. *J Cell Biol* **1005-15**
- Jones DL, Kochian LV (1997) Aluminum interactions with plasma membrane lipids and enzyme metal binding sites and its potential role in Al cytotoxicity. *FEBS* **400**: 51-7
- Jones DL, Kochian LV (1995) Aluminum inhibition of the inositol 1,4,5-trisphosphate signal transduction pathway in wheat roots: a role in aluminum toxicity? *The Plant Cell* **7**: 1913-22
- Kinkema M, Schiefelbein J (1994) A myosin from a higher plant has structural similarities to class V myosins. *J Mol Biol* **239**: 591-7
- Knight AE, Kendrick-Jones J (1993) A myosin-like protein from a higher plant. *J Mol Biol* **231**: 148-54

- Kohno T, Shimmen T (1988) Accelerated sliding of pollen tube organelles along *Characeae* actin bundles regulated by Ca^{2+} . *J Cell Biol* **106**: 1539-43
- Konishi S, Miyamoto S (1983) Alleviation of aluminum stress and stimulation of tea pollen tube growth by fluorine. *Plant Cell Physiol* **24**: 857-62
- Korn ED, Carlier MF, Pantaloni (1987) Actin polymerization and ATP hydrolysis. *Science* **238**: 638-44
- Lauffenburger DA, Horwitz AF (1996) Cell migration: a physically integrated molecular process. *Cell* **84**: 359-69
- Ma JF, Hiradate S, Nomoto K, Iwashita T, Matsumoto H (1997) Internal detoxification mechanism of Al in hydrangea. *Plant Physiol* **113**: 1033-9
- Macdonald TL, Humphreys WG, Martin RB (1987) Promotion of tubulin assembly by aluminum ion *in vitro*. *Science* **236**: 183-6
- Macdonald TL, Martin RB (1988) Aluminum ion in biological systems. *TIBS* **13**: 15-9
- Maciver SK, Wachsstock DH, Schwarz WH, Pollard TD (1991a) The actin filament severing protein actophorin promotes the formation of rigid bundles of actin filaments crosslinked with α -actinin. *J Cell Biol* **115**: 1621-8
- Maciver SK, Zot HG, Pollard TD (1991b) Characterization of actin filament severing by actophorin from *Acanthamoeba castellanii*. *J Cell Biol* **115**: 1611-20
- Matsudaira P (1991) Modular organization of actin crosslinking proteins. *TIBS* **16**: 87-92
- McLean BG, Eubanks S, Meagher RB (1990) Tissue-specific expression of divergent actins in soybean root. *The Plant Cell* **2**: 335-44
- Metcalf TN III, Wang JL, Schubert KR, Schindler M (1983) Lectin receptors on the plasma membrane of soybean cells. Binding and lateral diffusion of lectins. *Biochem* **22**: 3969-75
- Mitchison TJ, Cramer LP (1996) Actin-based cell motility and cell locomotion. *Cell* **84**: 371-9
- Pardee JD, Spudich JA (1982) Purification of muscle actin. *Meth Cell Biol* **24**: 271-89
- Pasternak C, Elson EL (1985) Lymphocyte mechanical response triggered by cross-linking surface receptors. *J Cell Biol* **100**: 860-72

- Pollard TD, Goldberg I, Schwarz WH (1992) Nucleotide exchange, structure, and mechanical properties of filaments assembled from ATP-actin and ADP-actin. *J Biol Chem* **267**: 20339-45
- Pollard TD, Cooper JA (1986) Actin and actin-binding proteins. A critical evaluation of mechanisms and functions. *Ann Rev Biochem* **55**: 987-1035
- Rengel Z (1992) Role of calcium in aluminum toxicity. *New Phytol* **121**: 499-513
- Ryan PR, Kinraide TB, Kochian LV (1994) Al^{3+} - Ca^{2+} interactions in aluminum rhizotoxicity I. Inhibition of root growth is not caused by reduction of calcium uptake. *Planta* **192**: 98-103
- Savory J, Huang Y, Herman MM, Wills MR (1996) Quantitative image analysis of temporal changes in tau and neurofilament proteins during the course of acute experimental neurofibrillary degeneration; non-phosphorylated epitopes precede phosphorylation. *Brain Res* **707**: 272-81
- Simon VR, Swayne TC, Pon LA (1995) Actin-dependent mitochondrial motility in mitotic yeast and cell-free systems: identification of a motor activity on the mitochondrial surface. *J Cell Biol* **130**: 345-54
- Sparling DW, Lowe TP (1996) Environmental hazards of aluminum to plants, invertebrates, fish, and wildlife. *Rev Env Con Tox* **145**: 1-128
- Walton J, Tuniz C, Fink D, Jacobsen G, Wilcox D (1995) Uptake of trace amounts of aluminum into the brain from drinking water. *Neurotox* **16**: 187-90
- Weiss C, Haug A (1987) Aluminum-induced conformational changes in calmodulin alter the dynamics of interaction with melittin. *Arch Biochem Biophys* **254**: 304-12
- Zaner KS, Valberg PA (1989) Viscoelasticity of F-actin measured with magnetic microparticles. *J Cell Biol* **109**: 2233-43

Chapter 2
OPTICAL DISPLACEMENT MICROVISCOMETRY (ODM)
AND ACTIN

ABSTRACT

A new method termed Optical Displacement Microviscometry (ODM) was developed to measure the viscosity of actin solutions in reconstituted microvolumes (10 μ L). This method utilizes a laser optical trap to displace a microbead within a microvolume of solution on a microscope slide. The power to displace the bead is found to be proportional to the viscosity of the solution. The method was shown to provide results that are comparable to those obtained utilizing capillary viscometry, but by using significantly less material. The technique was also used to perform a comparative analysis of the viscosity of purified F-actins isolated from rabbit muscle, human platelets, and maize pollen.

Chapter 2

OPTICAL DISPLACEMENT MICROVISCOMETRY (ODM) AND ACTIN

INTRODUCTION

In the early 1970's, Ashkin (1970) first demonstrated that a focussed beam of laser light could be utilized to "hold" or "trap" stationary and motile microscopic objects. The term "optical trapping" or "laser tweezers" was applied to this phenomenon. As light passes through these transparent structures and is refracted off the surfaces, momentum is transferred from the light to the object. In a light gradient, the vectoral sum of all the momentum transfers nudge the object into the region of maximum light intensity (the focal plane) where it remains trapped. Although this phenomenon is independent of excitation wavelength, infrared light sources have been most widely employed in biological systems since the least amount of photodamage was found to occur at these wavelengths during long term illumination (Ashkin, et al., 1987). Since the introduction of this method, optical trapping has been used for the following examinations: trapping of a single bacterium for investigations of flagella motor function (Block, et al., 1991), determination of the force and mechanisms of individual molecular motors (Ashkin, et al., 1990; Block, et al., 1990; Kuo and Sheetz, 1993; Simmons, et al., 1993; Molloy, et al., 1995; Nishizaka, et al., 1995; VanBuren, et al., 1995) or of

transcriptional complexes (Yin, et al., 1995); determining rigidity and flexibility of macromolecules such as DNA (Wang, et al., 1997) or cytoskeletal polymers (Simmons, et al., 1993; Felgner, et al., 1996); study of binding constants of different membrane glycoproteins to the cytoskeleton (Kucik, et al., 1991); inducing cell fusion with the aid of another laser (Steubing, et al., 1991); and monitoring induced changes within the cytoskeleton in living plant cells (Grabski and Schindler, 1995; Schindler, 1996).

A common parameter for each of these experiments is laser power. In most of the trapping experiments, the intensity of the laser beam is monotonically increased until a microscopic object can either be moved or held in place against an opposing force. The variations in laser power necessary to move micron sized objects within cells or through solutions can be used as a parameter to determine relative changes in solution structure, solution viscosity, and the organization of skeletal components that can bind to or interfere with the unhindered motion of these objects. The advantages of this technology for the performance of viscosity measurements within cells and model systems containing microliter volumes of solution suggested that optical trapping would be a most useful technique for the development of *in vitro* analytical systems. The method could examine the viscosity of the actin network under a variety of experimental conditions and in the presence of a number of actin binding proteins. This chapter of the dissertation describes the design and use of a new method termed Optical Displacement Microviscometry (ODM) to measure the viscosity of reconstituted actin solutions on microscope slides using samples as small as 10 μ l. These measurements are demonstrated to be comparable to more standard viscosity measurements performed with semi-micro-capillary viscometer. However, a significant advantage of the ODM for

biological investigations is that it requires far less sample than alternate methods. This chapter also reports the use of ODM for performing the first comparative measurements of viscosity on a purified plant actin, maize pollen actin. The successful use and characterization of this method provides researchers with a new tool to measure the viscosity of scarce biological samples and suggests the possibility of measuring viscosity changes at unique sites within living cells.

MATERIALS AND METHODS

Solutions. Buffer A, 2 mM Tris, pH 8.0 at 25° C, 0.2 mM Na₂-ATP, 0.2 mM CaCl₂, 0.5 mM 2-mercaptoethanol (βME); Buffer A⁺, Buffer A with 2 mM MgCl₂ and 50 mM KCl; Plant Buffer A, 5 mM Tris, pH 7.0, 0.2 mM Na₂-ATP, 0.2 mM CaCl₂, 0.5 mM βME, 0.005% NaN₃; Plant Buffer A⁺, Plant Buffer A with 2 mM MgCl₂ and 50 mM KCl; Sample Buffer, 10 mM Tris, pH 6.8, 10 % glycerol, 2 % SDS, 0.5 % βME, 0.1 mg/ml Bromophenol Blue.

Reagents. Rabbit muscle acetone powder was a generous gift from Dr. Steve Heidemann, Michigan State University, East Lansing, MI; human platelet actin was purchased from Cytoskeleton, Inc., Denver, CO; maize pollen actin was a generous gift of Dr. Chris Staiger, Purdue University, West Lafayette, IN; bovine plasma gelsolin, bovine serum albumin, commercial grade L-α-phosphatidylcholine, cytochalasin D, dimethyldichlorosilane, Folin-Ciocalteu's Phenol Reagent, imidazole, 2-mercaptoethanol, Na₂-ATP, NaN₃, and phalloidin were purchased from Sigma, St. Louis, MO; KCl, high performance liquid chromatography (HPLC)-grade methanol and MgCl₂ were purchased from J. T. Baker, Phillipsburg, NJ; CaCl₂ and DMSO were purchased from Mallinckrodt, St. Louis, MO; Tris Base and glycerol were purchased from Boehringer Mannheim, Indianapolis, IN; CuSO₄·5H₂O was purchased from Fisher, Fairlawn, NJ; Polybead[®] amino 1.0 micron microspheres were purchased from Polysciences, Warrington, PA, with additional polystyrene and glass bead samples a gift from Bangs Laboratories, Fisher, IN; 200 proof ethanol was purchased from Quantum Chemical Co., Insula, IL; Bodipy-phalloidin was purchased from Molecular Probes,

Eugene, OR; Rain X was manufactured by Unelko, Corp., Scottsdale, AZ; Permatex silicone spray was manufactured by Loctite Corp., Cleveland, OH.

Preparation of F-actin from Rabbit Muscle Acetone Powder. The following procedure is a modification of that of Pardee and Spudich (1982), as obtained from Dr. Steve Heidemann:

Two hundred ml of Buffer A at 4° C (2 mM Tris, pH 8.0 at 25° C, 0.2 mM Na₂-ATP, 0.2 mM CaCl₂, 0.5 mM 2-mercaptoethanol (βME)) was added to 10 g rabbit muscle acetone powder. Following 10 minutes of stirring, the solution was filtered through Whatman 543 paper. Residue was reextracted with 100 ml Buffer A and filtered. Combined filtrates were centrifuged for 60 minutes at 10⁴ g at 4° C in a Sorvall SS-34 rotor. Actin was assembled in a two step process: first MgCl₂ and KCl were added to concentrations of 0.7 mM and 10 mM, respectively, followed by a 60 minute incubation at 15° C; then MgCl₂ and KCl were added to final concentrations of 2 mM and 50 mM and incubation proceeded at 15° C for another hour.

Assembled F-actin was precipitated by a 2 hour spin at 1.5 x 10⁵ g at 4° C in a Beckman Ti60 rotor. Pellets were rinsed and overlaid with Buffer A and left to swell overnight. Swelled pellets were dispersed with a micropipettor and then sonicated for 3 x for 5 seconds each sonication. Sample volume was adjusted to 100 ml following addition of Na₂-ATP to 1 mM and CaCl₂ to 1 mM. Samples were dialyzed against 1 L Buffer A (3 x) for a total of 24 hours.

Dialyzed extract was centrifuged for 2 hours at 10⁵ g at 4° C in a Beckman Ti60 rotor. F-actin was reassembled in a two-step process as above. Polymerized actin was centrifuged for 2 hours at 1.5 x 10⁵ g in a Beckman Ti60 rotor. Pellets were

homogenized in F-actin stabilizing buffer (10 mM imidazole, 0.1 M KCl, 0.1 mM β ME, pH 7.0) and stored at 4° C in the presence of 10 μ M NaN₃.

Non-muscle and plant actin. Human platelet actin (Product #APH) was purchased from Cytoskeleton, Inc. It was diluted to 1 mg/ml in Buffer A (pH 8.0) and stored at 4° C immediately following arrival in the lab. Maize pollen actin was obtained as a gift from Dr. Chris Staiger of Purdue University. Both types of actin were diluted into appropriate sample buffer immediately prior to use.

Preparation of muscle actin for viscometry. F-actin was depolymerized by overnight microdialysis against Buffer A, and protein concentrations were determined by the method of Lowry, et al. (1951). G-actin was diluted to 1 mg/ml, and then repolymerization was initiated by the addition of KCl to 50 mM and MgCl₂ to 2 mM. Following polymerization at 15° C for 2 hours, actin was diluted into sample solutions which were mixed at 4° C and then incubated for 1 hour at room temperature, a time previously demonstrated to be adequate for cytochalasin D, phalloidin, and gelsolin to have their effect. Aliquots (15 μ l) were saved for confocal microscopy.

Cytochalasin D and phalloidin were dissolved in methanol or DMSO before dilution in Buffer A. Controls include the same concentration of methanol or DMSO as used in the sample solution.

Capillary viscometry. Relative viscosities were determined using a Cannon-Manning semi-micro capillary viscometer (Cannon Instrument Co., State College, PA). Time values were measured for the flowtime of a solution in a capillary tube, and relative viscosities were calculated by dividing the mean flow time for five trials by the mean flow time for a standard solution.

Optical displacement microviscometry (ODM). Polystyrene microspheres were diluted 1:10 with distilled water. One microliter of diluted beads was added to 15 μ l of sample solution, which was then placed on a lipid-coated microscope slide (see below) and sealed under a coverslip using melted paraffin as the sealant. A focused argon laser beam from an ACAS 570 Fluorescence Interactive Laser Cytometer (FILC) (Meridian Instruments, Okemos, MI) was used to optically trap suspended microspheres, and the laser power was monotonically increased until captured beads could be translocated through a defined distance. Values are given as relative viscosities, which are calculated by dividing the laser power necessary to translocate beads in the sample solution by that needed to move them in buffer alone. Plotted values are the mean of five trials, with error bars indicating standard deviation from the mean.

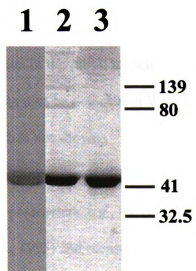
Preparation of microscope slides for ODM. To prevent the polystyrene microspheres from sticking to the microscope slides in high salt solutions, the slides were coated with a thin lipid layer. Five coats of commercial grade L- α -phosphatidylcholine (stock of 500 μ g/ml; 50 μ l each coat) in ethanol were applied in 8 minute intervals to precleaned, plain 3 x 1 inch microslides (VWR Scientific, Chicago, IL) in a humidity chamber, which consisted of an overturned dishpan containing a small tray filled with water and a sponge. Coated slides were allowed to dry overnight in the humidity chamber before use.

Visualization of actin filaments. An aliquot of each sample used in viscosity measurements was also examined using an Insight Bilateral Laser Scanning Confocal microscope (Meridian Instruments, Okemos, MI). One microliter of Bodipy-phalloidin (6.6 μ M) was added to 15 μ l of actin solution, resulting in a final concentration of 0.44

μ M Bodipy phalloidin. Actin stained with Bodipy-phalloidin was added to microscope slides and sealed under coverslips with melted paraffin.

SDS-PAGE analysis. Two micrograms of protein were suspended in Sample Buffer and boiled for 2'. Proteins were loaded onto a 10% SDS polyacrylamide gel with a stacking gel (Laemmli, 1970) and electrophoresed for 1 hour at a constant voltage of 200 volts to assay for purity (Figure 1). Proteins were visualized by staining overnight with Coomassie Brilliant blue stain; gels were destained with a 1:1 solution of methanol/acetone, and then equilibrated for one hour with fifty percent methanol in water and dried onto cellophane.

Figure 1. SDS-PAGE of actin samples. Two micrograms of rabbit muscle actin (Lane 1), maize pollen actin (Lane 2), and human platelet actin (Lane 3), respectively, were electrophoresed on SDS-PAGE gels and stained with Coomassie Brilliant blue as described in materials and methods. Molecular weights are listed in kilodaltons.



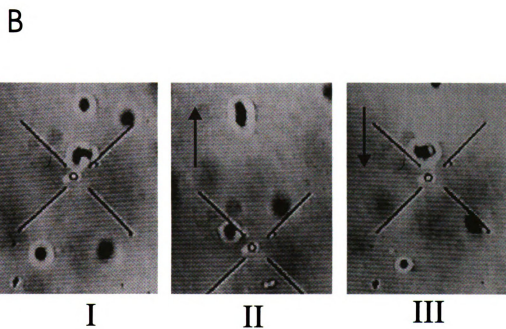
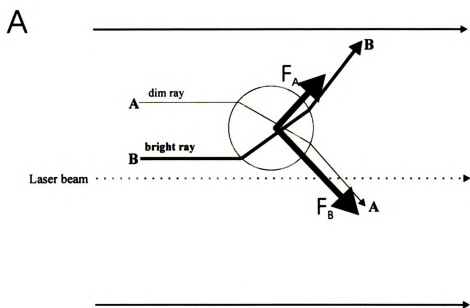
RESULTS

SDS-PAGE of protein samples. The purity of proteins studied in this chapter was examined with SDS-PAGE. Samples of maize pollen actin, rabbit muscle actin, and human platelet actin were electrophoresed and then stained with Coomassie Brilliant blue (Figure 1). Although each lane contained only one prominent band, some higher molecular weight bands can be seen in the rabbit muscle actin (Lane 2). However, these higher molecular weight bands can also be detected in Western blots using antibodies specific for rabbit muscle actin (data not shown).

Optical Displacement Microviscometry (ODM). Optical trapping has been used to examine a number of physical parameters, e.g., measurements of the force generated by a myosin motor (Miyata, et al., 1995) and measurements of tension within the actin network of soybean root cells (Grabski and Schindler, 1995). These diverse experimental designs all depend on the same physical principle which is shown in a schematic diagram (Figure 2A). Light provided by a laser passes through a transparent object and is refracted at the air/solid interface. Since light has momentum as defined by the DeBroglie relationship, each ray of light that is refracted transfers momentum from itself to the object resulting in a force on the object. In the case of the two rays shown, both will alter the momentum of the particle; however, the beam of higher intensity (**B**) contains more photons and will thus have a greater effect upon the bead. A laser beam with a gradient of intensities will pull the object toward the center of the beam (the focal plane). Physical measurements can be made by comparing the laser power necessary to trap objects under varying conditions.

Figure 2. Optical trapping of polystyrene microspheres. A schematic representation of the physical principles of optical trapping (A). Rays passing through a polystyrene bead are refracted at incident surfaces. The bead will experience a change of momentum equal in magnitude but opposite in direction to that of the photons it is refracting (F_A & F_B). Since rays of higher intensity will have a greater effect than those with a lower intensity, the bead will be pulled into the middle of a light gradient.

A polystyrene bead (1.0 micron in diameter) is optically trapped (bead in cross-hairs) (first panel) and the stage is translated (in the direction of the arrow) (second and third panel) resulting in the displacement of the bead from the original position (B).



Optical trapping seems well-suited for viscosity measurements. A simple definition of viscosity is resistance to flow. An object in a highly viscous solution will be exposed to much greater resistance to flow than one in a solution of low viscosity. With an optical trap, the higher the viscosity, the greater the laser power necessary to trap and displace an object within the solution. Differences in viscosity should result in significant differences in laser power needed for trapping.

Figure 2B demonstrates the translocation of a polystyrene bead on a microscope slide. Polystyrene beads (Polysciences, Inc.; polystyrene and glass beads from Bangs Laboratories were also evaluated, with no significant differences in bead performance) are suspended within a solution and placed on a microscope slide. A single bead (in cross-hairs, **(I)**) is trapped with a focused argon laser beam at a wavelength of 488 nm. The microscope stage is translated a defined distance at constant velocity in the direction of the arrow as the bead is held within the trap **(II)**. The bead can then be returned to its original position (translation of stage indicated by arrow, **(III)**). The intensity of the beam is adjusted to determine the minimum power necessary to maintain the bead in the trap as the slide is displaced.

Optical Displacement Microviscometry measurements were compared using identical samples with data obtained from a capillary viscometer, a commonly employed method for measuring the viscosity of solutions (Figure 3). Increases in glycerol concentration correlate with increases in relative viscosities as measured by both techniques. The nearly identical curves observed for both techniques verify that ODM is a comparable method for measuring the viscosity of glycerol solutions. The use of the ODM, however, provides a number of advantages. First, ODM measurements can utilize

sample volumes as small as 10 μl , in contrast to the 500 μl of sample necessary for the capillary viscometry measurements. Secondly, ODM can measure changes of viscosity within microdomains of samples, rather than from bulk solution measurements as obtained with the capillary viscometer.

Since actin polymerization depends on millimolar concentrations of magnesium and potassium, the assay must be optimized while maintaining these salt concentrations. High concentrations of salt were found to promote bead aggregation on the surface of the microscope slides; this interferes with trapping experiments using F-actin solutions. A number of approaches were attempted to circumvent this problem, resulting in varying levels of success. Bead aggregation was independent of bead manufacturer, type (polystyrene or glass), or charge. Blocking of beads with bovine serum albumin, cytochrome C, or casein also proved unsuccessful, as were attempts to coat either the beads or the slides with Rain X, silicone spray, or dimethyldichlorosilane. However, a new approach, coating the slides with phospholipid, proved to be satisfactory. Combinations of phosphatidylcholine, phosphatidylserine, and phosphatidylethanolamine in methanol, ethanol, acetone, and chloroform were examined to see if aggregation could be prevented (data not shown). Best results were obtained with 500 $\mu\text{g/ml}$ phosphatidylcholine in ethanol. It was also found that coating the slides with lipid was most successful when they were maintained in a high humidity chamber throughout the process.

ODM of actin solutions. Stock rabbit muscle F-actin (1 mg/ml) was diluted in Buffer A⁺ and incubated for 1 hour at room temperature. Relative viscosities were determined for a range of actin concentrations using ODM (Figure 4). An increase in

Figure 3. Comparison of capillary viscometry with Optical Displacement Microviscometry (ODM). Measurements of the relative viscosity for increasing concentrations of glycerol were obtained by capillary viscometry (■) and ODM (♦).

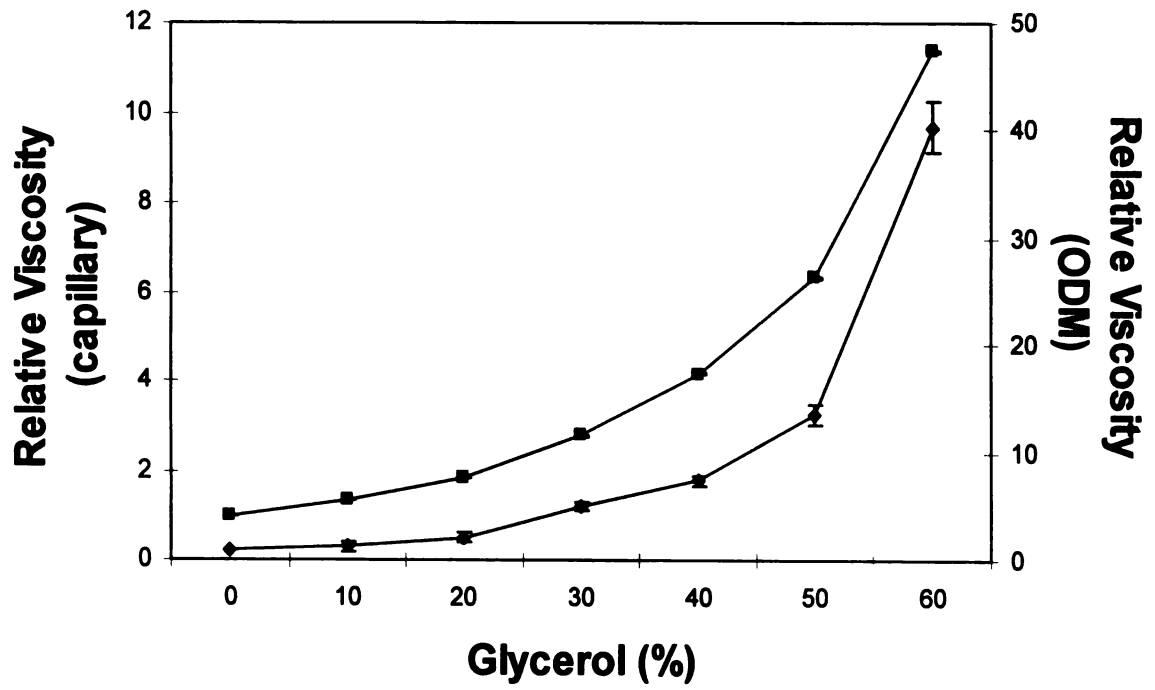
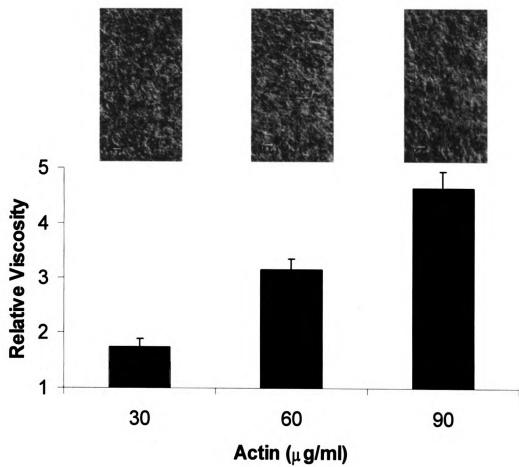


Figure 4. ODM measurements performed on solutions of rabbit muscle F-actin . F-actin was diluted into Buffer A⁺ and then evaluated with ODM. Confocal fluorescence images of an aliquot of each of the actin concentrations were stained and examined with Bodipy-phalloidin as described in materials and methods.



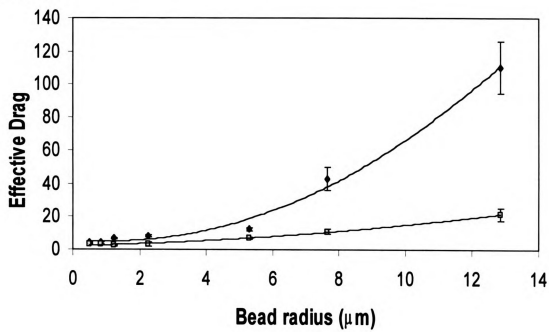
actin concentration led to a corresponding monotonic increase in relative viscosity over the range of actin concentrations. Above actin concentrations of 400 $\mu\text{g/ml}$ the laser power necessary to translocate the beads was so great that it heated the beads excessively, which resulted in their destruction (opticalcution). Actin concentrations were well above the critical concentration of 0.1 μM (4.2 $\mu\text{g/ml}$), as evidenced by the images of actin filaments obtained with a laser scanning confocal fluorescence microscope (Figure 4). These data indicate that ODM is capable of measuring differences in the viscosity of F-actin solutions over a three-fold range of actin concentrations.

Bead radius and effective drag. Movement of beads in actin solutions was found to be dependent upon their surface area. The size dependency for beads translated through actin solutions was evaluated by measuring the trapping intensity necessary to maintain different sized microbeads within a trap in 60 $\mu\text{g/ml}$ solutions of actin (Figure 5A). Since the actual viscosity of the solution was identical for all the data points, values for the differences in measurements which were determined utilizing the displacement of beads of varying size are given as changes in “effective drag.” For comparison, cytochalasin D, a fungal cytotoxin that depolymerizes F-actin, was added to the F-actin solutions to reduce the solution structure. Significant drops in effective drag were observed, though values still increased with increasing bead size. Even though solutions contained the same actin concentration, drag differed depending upon the degree of actin polymerization. This indicates that differences in the organization of the actin can also be detected with ODM. Similar results were obtained by Janson and Taylor (1993), who found that velocities of polystyrene beads propelled as a result of gel contraction depended upon the solution of the actin filament network. Upon activation of the

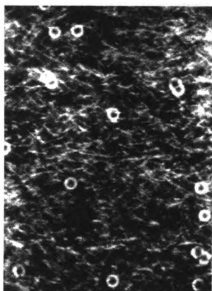
Figure 5. An evaluation of the effective drag as a function of bead radius.

Microspheres having different radii were trapped and translocated in a solution of rabbit muscle F-actin (60 $\mu\text{g/ml}$) in the absence (\blacklozenge) and presence (\blacksquare) of 1 μM cytochalasin D (A). Confocal fluorescence image of 1.0 micron beads in a network of actin filaments (B).

A



B

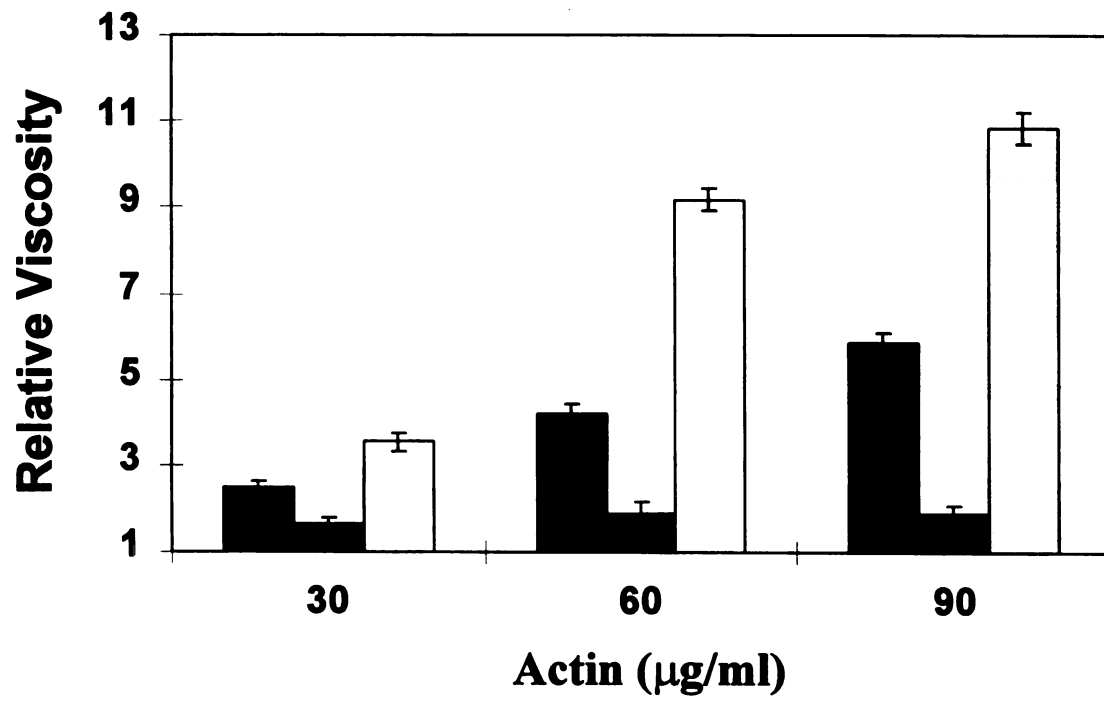


severing activity of gelsolin, bead velocity increased dramatically as a result of decreased fluid structure and contraction of actin gels.

Confocal fluorescence images show beads of different size within an F-actin network (Figure 5B; note the 1 μm beads suspended in the actin mesh). Both curves are best characterized using a second order best fit. Such relationships were similarly observed by Hou et al (1990). In studying the diffusion of inert particles in actin solutions, Hou and colleagues noted that changes in the structure of actin solutions could be detected as alterations in Brownian motion of labeled Ficoll (Hou, et al., 1990). They found that an inverse relationship existed between solution density and the size of particles which were able to freely diffuse. Diffusion through actin networks appeared to be related to the cross-sectional area of the particle with a similar power dependency as was observed in the ODM measurements. These observations can be interpreted to provide experimental evidence for the theoretical relationship between effective drag and the surface area of the microsphere or macromolecule.

Effects of cytochalasin D and phalloidin. Two fungal cytotoxins, phalloidin and cytochalasin D, alter F-actin organization, and thereby affect the viscosity of actin solutions (Cooper, 1987). Phalloidin binds tightly to F-actin, stabilizing it against depolymerization. Conversely, cytochalasin D induces the depolymerization of F-actin, decreasing the viscosity of actin solutions. These alkaloids have been widely used in the study of actin. Samples of F-actin were mixed and incubated with either cytochalasin D or phalloidin at 4° C and suspended on a microscope slide. ODM measurements of phalloidin-treated samples demonstrated that higher laser powers were necessary to translocate the beads, indicating a higher viscosity (Figure 6). In contrast and as

Figure 6. Effects of fungal alkaloids on the viscosity and organization of F-actin. ODM measurements of muscle actin in the presence of cytochalasin D (2 μ M, black bars), phalloidin (2 μ M, white bars), and incubation buffer (gray bars).



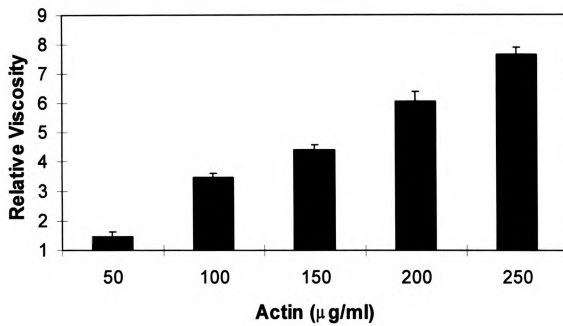
predicted, cytochalasin D reduced the laser intensity necessary to move the bead through the F-actin solution (Figure 6).

Non-muscle actin. Human platelet actin was diluted in Buffer A⁺ and relative viscosities were determined over a range of concentrations. As observed with rabbit muscle actin, increases in actin concentration corresponded to monotonic increases in relative viscosity measurements (Figure 7A). Confocal fluorescence microscopy confirmed the presence of a dense actin filament network in 200 µg/ml solutions. (Figure 7B). The high filament density is quite noticeable, showing the enhanced potential for interactions between filaments which would result in increases in the viscosity of the solution. These data show that ODM can measure differences in viscosities for both muscle and non-muscle actin solutions and that both types of actin demonstrate similar changes in viscosity as a function of F-actin concentration.

Plant actin. Maize pollen actin was diluted into Plant Buffer A⁺ and incubated at room temperature for 1 hour. Microviscosity measurements with maize pollen actin demonstrate that increases in actin concentration correspond to increases in the relative viscosity sensed by a microbead displaced through the actin solution (Figure 8A), just as previously observed with rabbit muscle and human platelet actin. However, the extent of increase of viscosity for plant actin is significantly less, a result which may suggest a higher critical concentration for plant actin or differences in physical properties such as flexibility or rigidity. Confocal fluorescence microscopy showed dense solutions of actin (Figure 8B), suggesting that the latter may be more likely. Though samples of maize pollen actin proved more difficult to interpret than the other actins, a trend in increasing viscosity was noted toward denser solutions of actin.

Figure 7. Measurements of the viscosity and organization of F-actin purified from human platelets. ODM measurements were performed with solutions of human platelet derived F-actin (A). Confocal fluorescence image of the organization of human platelet F-actin (150 $\mu\text{g/ml}$) (B).

A



B

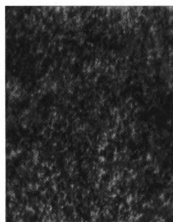
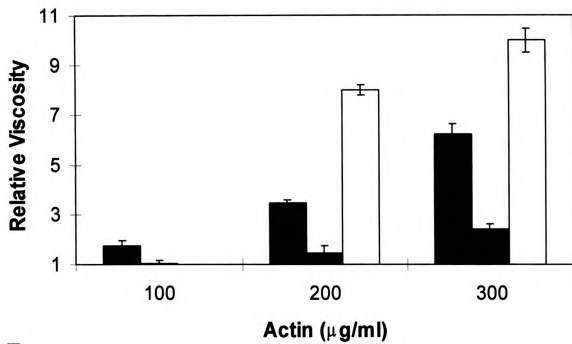
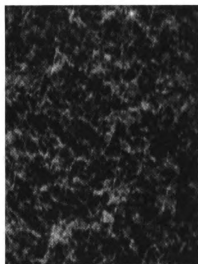


Figure 8. Measurement of the viscosity and organization of F-actin purified from maize pollen. ODM measurements of F-actin isolated from maize pollen in the presence of buffer (gray), cytochalasin D (7 μ M, black bars), or phalloidin (7 μ M, white bars) (A). Confocal fluorescence image of F-actin isolated from maize pollen (100 μ g/ml) (B).

A



B



Maize pollen actin was also incubated with cytochalasin D and phalloidin. As shown with muscle actin, cytochalasin D disrupted plant F-actin, noticeably lowering solution viscosities (Figure 8A). Dramatic increases in viscosities were observed upon incubation with phalloidin. These are the first comparative *in vitro* physical measurements of a plant type actin and show that viscosity is modified in response to fungal cytotoxins in the same manner as observed for other F-actin types. This suggests that the physical properties and structure of plant actin is probably very similar to the animal and yeast types.

Measurements of actin organization and viscosity. Actin filament length can be altered by the addition of toxins that are capable of changing the degree of polymerization as described above for phalloidin and cytochalasin D. However, cells can modulate their own F-actin length through the expression of proteins such as gelsolin, a 90 Kda protein which can sever and cap actin filaments following the addition of Ca^{2+} (Bearer, 1991). Changes in filament length which have been induced by gelsolin should be quantifiable through viscosity measurements. The severing of actin filaments by gelsolin was studied *in vitro* with confocal fluorescence microscopy and optical displacement microviscometry. Addition of calcium initiated severing of actin by gelsolin, lowering effective viscosities (Figure 9A). Actin samples without gelsolin showed little variation from control with increasing amounts of Ca^{2+} .

Confocal fluorescence imaging of gelsolin-treated samples provide independent support for the ODM measurements. Long, distinct actin filaments could be seen in images obtained with samples that also demonstrated high viscosity using the ODM (Figure 9B). Few distinguishable actin filaments are visible in samples demonstrating

Figure 9. The effect of gelsolin in the absence and presence of calcium on the viscosity and organization of rabbit muscle F-actin. Six milliunits of gelsolin were added to rabbit muscle F-actin (100 $\mu\text{g}/\text{ml}$). Upon addition of 5.0 mM calcium (black bars), gelsolin severing activity greatly diminished F-actin solution viscosity (A). Confocal fluorescence images of actin and gelsolin in the absence (first panel) and presence of 5.0 mM calcium (second panel) (B).

low viscosity. Rather, a lawn of indistinct actin staining accompanies these samples, consistent with an abundance of short filaments generated by severing of longer filaments.

DISCUSSION

A new technique has been developed for the measurement of viscosity within cells and micro-solutions. These measurements can be used to examine changes in the organization and assembly of actin solutions in the absence and presence of actin binding proteins and other actin effector molecules. A significant advantage of the method is that viscometric measurements can be performed in volumes as small as 10 μ l.

At the time this work was initiated, a sample of purified plant actin was only available in extremely small amounts. These amounts were below the quantities necessary for accurate physical characterization by available means. For this reason, it became necessary to develop a more sensitive type of viscometric assay that could provide accurate measurements utilizing small amounts of material. Since the laboratory had pioneered the use of optical trapping for *in vivo* measurements of the viscoelastic properties of F-actin filaments in living plant cells, it was determined that the optical trapping technology could be modified to perform related viscosity measurements in micro-solutions.

The first experiments showed that polystyrene microspheres could be trapped on a microscope slide. Subsequent addition of beads to glycerol solutions confirmed that optical trapping could be used to detect viscosity differences between samples. The shape and dependency of the curves obtained using both the ODM and capillary viscometer were identical, and showed that the new technique could provide comparable results using only 15 μ l of sample. This reduced sample consumption by more than an

order of magnitude from more conventional measurement protocols. Optical Displacement Microviscometry (ODM) was validated as a technique to detect differences in solution viscosities.

For ODM to be of any value in our studies, it would have to function with biological samples and under the conditions required for their maintenance. Considerable manipulation of experimental conditions allowed the collection of data using different concentrations of rabbit muscle actin. The greater the meshwork of actin filaments present, the more laser power was necessary to trap and translocate the polystyrene beads. Alteration of the filament length by addition of phalloidin and cytochalasin D revealed that filament structure, in addition to protein concentration, was important for solution viscosity and could be measured with our assay. The assay demonstrated that it could be used to detect biologically relevant data relating to the structure of actin filaments *in vitro*. Coupled with the use of laser scanning confocal fluorescence microscopy, this new technique has the potential to determine minute changes in actin filament networks in microvolumes upon addition of other proteins, ions, or toxins.

A further validation of this technique was obtained measuring effective drag using beads of increasing diameter in actin in the absence or presence of cytochalasin D. In the presence of cytochalasin D, increases in laser power are required to translocate a bead with increasing diameter. Larger, more massive polystyrene microspheres require greater laser power to trap and displace them. Without cytochalasin D, this effect is even more exaggerated. Beads interact with actin filaments, creating resistance to translocation and increasing their effective drag. The gelsolin data further confirm these findings.

Curves from the graphs comparing bead size with viscosity are best fit by a

second order equation, providing experimental support for the theoretical relationship between measured viscosity and the square of the bead diameter. One can easily imagine that if a solution is perceived as a molecular sieve, the larger the cross-section of an object, the more difficult will be its journey through the solution. Dependence of the cross-sectional area on measured viscosity suggests that: a) the beads are only affected by spatial considerations, rather than chemical interactions with the solution, and b) that slight differences in solution structure can be detected with this method.

These results provide the experimental foundation for this new method as a means to measure the viscosity in the absence and presence of signaling agents, ions, and cellular effectors within subcompartments of living cells. The use of particle guns to shoot microbeads into cells could provide an opportunity to examine structural changes and molecular interactions within different domains of the cytoplasm in a single cell. ODM provides another tool for study of organization of the cytoskeleton *in vitro* and *in vivo*.

The small sample size required for the assay permits physical measurements to be performed using scarce biological materials, in volumes previously too small to analyze. To the best of our knowledge, the comparative measurements of viscosity between plant actin, rabbit muscle, and a non-muscle actin (human platelet F-actin) are the first such measurements to be performed. This comparison suggests that plant actin has much the same physical properties as the animal and yeast counterparts, although it does not appear to polymerize as well. Further refinement of the assay will enable us to monitor similarities and differences in these isotypes upon addition of different actin-binding proteins.

REFERENCES

- Ashkin A (1970) *Phys Rev Let* **24**: 156
- Ashkin A, Dziedzic JM (1987) Optical trapping and manipulation of viruses and bacteria. *Science* **235**: 1517-20
- Ashkin A, Dziedzic JM, Yamane T (1987) Optical trapping and manipulation of single cells using infrared laser beams. *Nature* **330**: 769-71
- Ashkin A, Schutze K, Dziedzic JM, Euteneuer U, Schliwa M (1990) Force generation of organelle transport measured in vivo by an infrared laser trap. *Nature* **348**: 346-8
- Bearer EL (1991) Direct observation of actin filament severing by gelsolin and binding by gCap39 and CapZ. *J Cell Biol* **115**: 1629-38
- Block SM (1992) Making light work with optical tweezers. *Nature* **360**: 493-5
- Block SM, Blair DF, Berg HL (1991) Compliance of bacterial polyhooks measured with optical tweezers. *Cytometry* **12**: 492-6
- Block SM, Goldstein SB, Schnapp BJ (1990) Bead movement by single kinesin molecules studied with optical tweezers. *Nature* **348**: 348-52
- Cooper JA (1987) Effects of cytochalasin and phalloidin on actin. *J Cell Biol* **105**: 1473-78
- Felgner H, Frank R, Schliwa M (1996) Flexural rigidity of microtubules measured with the use of optical tweezers. *J Cell Sci* **109**: 509-16
- Grabski S, Schindler M (1995) Aluminum induces rigor within the actin network of soybean cells. *Plant Physiol* **108**: 897-901
- Grabski S, Schindler M (1996) Auxins and cytokinins as antipodal modulators of elasticity within the actin network of plant cells. *Plant Physiol* **110**: 965-70
- Grabski S, Xie XG, Holland JF, Schindler M (1994) Lipids trigger changes in the elasticity of the cytoskeleton in plant cells: a cell optical displacement assay for live cell measurements. *J Cell Biol* **126**: 713-26
- Hou L, Lanni F, Luby-Phelps K (1990a) Tracer diffusion in F-actin and ficoll mixtures. Toward a model for cytoplasm. *Biophys J* **58**: 31-43
- Hou L, Luby-Phelps K, Lanni F (1990b) Brownian motion of inert tracer macromolecules in polymerized and spontaneously bundled mixtures of actin and filamin. *J Cell Biol* **110**: 1645-54

- Kucik DF, Kuo SC, Elson EL, Sheetz MP (1991) Preferential attachment of membrane glycoproteins to the cytoskeleton at the leading edge of lamella. *J Cell Biol* **114**: 1029-36
- Kuo SC, Sheetz MP (1993) Force of single kinesin molecules measured with optical tweezers. *Science* **260**: 232-4
- Laemmli UK (1970) Cleavage of structural proteins during the assembly of the head of bacteriophage T4. *Nature* **227**: 680-5
- Lowry OH, Rosenburg NJ, Farr AL, Randall RJ (1951) Protein measurement with Folin phenol reagent. *J Biol Chem* **193**: 265-75
- Molloy JE, Burns JE, Kendrick-Jones J, Tregear RT, White DCS (1995) Movement and force produced by a single myosin head. *Nature* **378**: 209-12
- Nishizaka T, Miyata H, Yoshikawa H, Ishiwata S, Kinoshita K Jr (1995) Unbinding force of a single motor molecule of muscle measured using optical tweezers. *Nature* **377**: 251-4
- Pardee JD, Spudich JA (1982) Purification of muscle actin. *Meth Cell Biol* **24**: 271-89
- Schindler M (1995) The cell optical displacement assay (CODA): measurements of cytoskeletal tension in living plant cells with a laser optical trap. *Meth Cell Biol* **49**: 69-82
- Simmons RM, Finer JT, Warrick HM, Kralik B, Chu S, Spudich JA (1993) Force on single actin filaments in a motility assay measured with an optical trap. *Adv Exp Med Biol* **332**: 331-7
- Steubing RW, Cheng S, Wright WH, Numajiri Y, Berns MW (1991) Laser induced cell fusion in combination with optical tweezers: the laser cell fusion trap. *Cytometry* **12**: 505-10
- VanBuren P, Guilford WH, Kennedy G, Wu J, Warshaw DM (1995) Smooth muscle myosin: a high force-generating molecular motor. *Biophys J* **68**: 256S-58S
- Wang MD, Yin H, Landick R, Gelles J, Block SM (1997) Stretching DNA with optical tweezers. *Biophys J* **72**: 1335-46
- Yin H, Wang MD, Svoboda K, Landrick R, Block SM, Gelles J (1995) Transcription against an applied force. *Science* **270**: 1653-7

Chapter 3

ALUMINUM AND THE ACTIN NETWORK

ABSTRACT

Optical Displacement Microviscometry (ODM) was used to examine the viscosity of solutions of actin purified from rabbit muscle, human platelets, and maize pollen. These measurements were performed in the presence and absence of aluminum to determine the effect of aluminum on the organization and viscosity of the actin solutions as well as whether there were differences between the different actin types. Similar experiments were then performed with solutions containing actin and either myosin or filamin, two proteins which crosslink actin filaments. The addition of micromolar concentrations of aluminum significantly increased the viscosity of actin solutions comprised of either of the three types of actin, but only in the presence of one of the actin cross-linking proteins. Analysis of *in vitro* viscosity measurements in conjunction with confocal fluorescence imaging of the actin solutions suggests that the ability of aluminum to aggregate F-actin filaments is significantly enhanced in the presence of cross-linking proteins.

Chapter 3

ALUMINUM AND THE ACTIN NETWORK

INTRODUCTION

The role of aluminum in the inhibition of plant growth has been investigated for over fifty years (Delhaize and Ryan, 1995; Sparling and Lowe, 1996). Though the soil is rich in aluminum, most of the aluminum is insoluble, bound to aluminosilicates and clays or chelated by phosphates and organic acids (Macdonald and Martin, 1988; Sparling and Lowe, 1996). As the pH of soil decreases, however, aluminum solubility increases (Macdonald and Martin, 1988; Sparling and Lowe, 1996), and the biologically active form, Al^{3+} , is released into the soil and groundwater (Macdonald and Martin, 1988). The economic impact of this release of free aluminum can be considerable, as crop productivity may be decreased by as much as 50%. (Delhaize and Ryan, 1995; Flaten, et al., 1996). Though aluminum has been suggested to affect a number of physiological processes in both plants and animals, the biochemical mechanism(s) of aluminum toxicity remain elusive (Delhaize and Ryan, 1995).

Recently, experiments from our laboratory demonstrated an entirely new activity for aluminum in plant cells (Grabski and Schindler, 1995). Utilizing a new technique developed in the laboratory (Grabski and Schindler, 1995), it was observed that following the addition of micromolar amounts of aluminum to soybean root cells grown in acidic

media (pH 5.8), the actin fibers within the transvacuolar strands dramatically changed their viscoelastic properties, becoming more rigid. The aluminum effect required acidic pH, occurred in less than 30 minutes, and was specific to aluminum. Other metallic cations, such as beryllium, barium, and lanthanum, did not cause similar changes. This chapter of the dissertation describes the methods, approaches, and results of investigations to determine the mechanism of aluminum activity within a model system composed of either F-actin filaments or F-actin filaments in the presence of actin binding proteins.

Chapter Two described the development and use of Optical Displacement Microviscometry (ODM), a sensitive new technique which incorporates the use of an optical trap to perform viscosity measurements within small volumes of sample (<10 μ l). In this chapter, ODM is utilized to examine actin filaments isolated from rabbit muscle, human platelets, and maize pollen in the presence of metallic cations and actin binding proteins in order to determine the effects of aluminum on the solution structure and viscosity of F-actin. Characterization of the *in vitro* data suggests that it effectively corresponds to results obtained from intact plant cells. A comparison of the *in vivo* and *in vitro* experiments provides the basis for a model for aluminum mediated changes within the actin network.

The degree of viscoelasticity of a bundle of actin filaments depends upon the extent of interaction between the filaments, the size of the filaments, and the nature of the crosslinkers (Waschsstock, et al., 1994). Alteration of these interactions by an agent such as a polyvalent cation would alter the ability of the filament bundles to resist outside forces. Likewise, any change in crosslinking within the filament bundles would be

evidenced by a change of viscosity. Therefore, viscosity changes in solution may be related to viscoelastic behavior. This relationship can be utilized to compare *in vitro* with *in vivo* measurements and should help provide the data necessary to prepare a model for Al^{3+} -induced changes in the cytoskeleton.

MATERIALS AND METHODS

Solutions. Buffer A, 2 mM Tris, pH 8.0 at 25° C, 0.2 mM Na₂-ATP, 0.2 mM CaCl₂, 0.5 mM 2-mercaptoethanol (β ME); Buffer A⁺, Buffer A with 2 mM MgCl₂ and 50 mM KCl; Luminometer Reaction Buffer, 50 mM Tris pH 7.8, 5 mM MgSO₄, 0.5 mM EDTA, and 0.5 mM BSA; Myosin ATPase Reaction Buffer, 20 mM Tris (pH 5.8), 50 mM KCl, 2 mM MgCl₂, and 200 μ M or 1 mM ATP; Plant Buffer A, 5 mM Tris, pH 7.0, 0.2 mM Na₂-ATP, 0.2 mM CaCl₂, 0.5 mM β ME, 0.005% NaN₃; Plant Buffer A⁺, Plant Buffer A with 2 mM MgCl₂ and 50 mM KCl; Sample Buffer, 10 mM Tris, pH 6.8, 10 % glycerol, 2 % SDS, 0.5 % β ME, 0.1 mg/ml Bromophenol Blue.

Reagents. Rabbit muscle acetone powder was a generous gift from Dr. Steve Heidemann, Michigan State University, East Lansing, MI; human platelet actin was purchased from Cytoskeleton, Inc., Denver, CO; maize pollen actin was a generous gift of Dr. Chris Staiger, Purdue University, West Lafayette, IN; β -galactosidase was a gift from Dr. William Smith, Michigan State University; bovine serum albumin, commercial grade L- α -phosphatidylcholine, cytochalasin D, chicken gizzard filamin, Folin-Ciocalteu's Phenol Reagent, imidazole, 2-mercaptoethanol, LaCl₃·7H₂O, luciferin-luciferase, bovine muscle myosin II, Na₂-ATP, NaF, NaN₃, and ZnCl₂ were purchased from Sigma, St. Louis, MO; AlCl₃·6H₂O and BeCl₂, were purchased from Aldrich, Milwaukee, WI; CuCl₂ and CuSO₄·5H₂O were purchased from Fisher, Fair Lawn, NJ; EDTA·Na₂, KCl, high performance liquid chromatography (HPLC)-grade methanol, MgCl₂, and trichloroacetic acid, were purchased from J. T. Baker, Phillipsburg, NJ; CaCl₂, DMSO, and FeCl₃·6H₂O were purchased from Mallinckrodt, St. Louis, MO; Tris

Base was purchased from Boehringer Mannheim, Indianapolis, IN; $\text{MgSO}_4 \cdot 7\text{H}_2\text{O}$ was purchased from Columbus Chemical Industries, Columbus, WI; Latrunculin B was purchased from LCL Laboratories, Woburn, MA; Polybead[®] amino 1.0 micron microspheres were purchased from Polysciences, Warrington, PA; 200 proof ethanol was purchased from Quantum Chemical Co., Insula, IL; and Bodipy-phalloidin was purchased from Molecular Probes, Eugene, OR.

Preparation of F-actin. F-actin from rabbit muscle, human platelets, and maize pollen was prepared as described in Chapter Two.

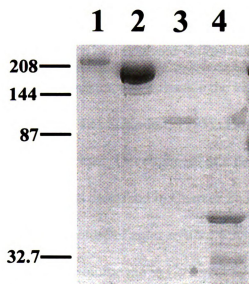
Techniques. Capillary viscometry, Optical Displacement Microviscometry (ODM), preparation of microscope slides, visualization of actin filaments, SDS-PAGE, and protein determination were performed as in Chapter Two.

Preparation of samples. Ions (100 mM stock) were diluted with F-actin to final concentration in appropriate sample buffer and incubated at room temperature for one hour. Myosin and filamin were equilibrated with F-actin at room temperature for 30 minutes before any experimental ions were added to their solutions. Further experimental conditions are provided in the experimental description.

Myosin ATPase assays. Samples were prepared in 20 mM Tris (pH 5.8), 50 mM KCl, 2 mM MgCl_2 , and 200 μM or 1 mM ATP. Actin concentration was 200 $\mu\text{g}/\text{mL}$. ATP hydrolysis was initiated by addition of bovine muscle myosin II to 10 milliunits/mL following addition of all other reagents. Samples were mixed and 2 μL aliquots were immediately removed and quenched by addition to 2 μL of ice-cold 7% trichloroacetic acid (final 3.5% of TCA). After 30', another 2 μL aliquot was removed and quenched with ice-cold TCA.

ATP content was assayed with a Turner TD-20e Luminometer (Turner Designs, Sunnyvale, CA). Twenty microliters of luciferin-luciferase solution (product # FL-AAM) were pipetted into the sample tube containing 4 μ l of quenched ATP reaction solution. One hundred sixteen microliters of Luciferase Reaction Buffer (50 mM Tris pH 7.8, 5 mM MgSO_4 , 0.5 mM EDTA, and 0.5 mM BSA) were next added and mixed, and 100 μ l of this solution was injected into the luminometer. At time zero the sample solution was mixed with the assay solution, and after 15" the light intensity was integrated over a 30" span.

Figure 1. SDS-PAGE of actin and actin binding proteins. SDS-PAGE gels were loaded with two micrograms of filamin (lane 1), myosin (lane 2), gelsolin (lane 3), and rabbit muscle actin (Lane 4), and electrophoresis was performed as described in materials and methods. Proteins were stained with Coomassie Brilliant blue. Molecular weights are given in kilodaltons.



RESULTS

Purity of proteins. The purity of the actin-binding proteins studied in this chapter was assayed by SDS-PAGE. Coomassie Brilliant blue staining of electrophoresed samples of chicken gizzard filamin, bovine muscle myosin, human platelet gelsolin, and rabbit muscle actin samples revealed one predominant band for each lane (Figure 1), verifying the purity of the samples.

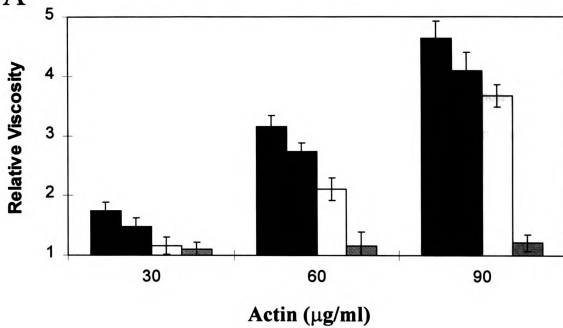
Effect of aluminum on actin polymerization and structure. Previous work in this laboratory showed that aluminum can influence the viscoelasticity of actin strands in soybean root cells (Grabski and Schindler, 1995). However, the mechanism of this aluminum effect is not yet clear. Development of a new assay, Optical Displacement Microviscometry (ODM) (as described in Chapter 2), has provided an *in vitro* method to examine changes in the structure of actin solutions induced by aluminum.

ODM was used to examine the *in vitro* effects of aluminum on the physical properties of actin filaments. Low concentrations of AlCl_3 had little effect on solution viscosity (Figure 2A). Addition of Al^{3+} to $200 \mu\text{M Al}^{3+}$, however, reduced solution viscosities to nearly baseline levels. Although intriguing, these results were difficult to interpret in the context of the *in vivo* data which show a direct effect of relatively low concentrations of Al^{3+} on the tension within actin filaments.

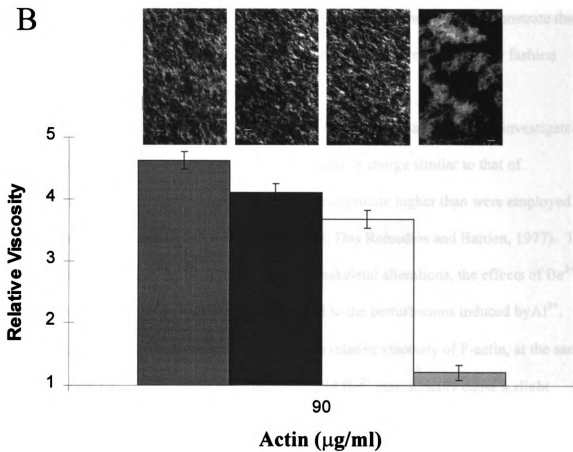
Confocal fluorescence microscopy provides another tool for evaluating changes in actin filament organization under different incubation conditions. F-actin filaments polymerized in the presence of $200 \mu\text{M Al}^{3+}$ appeared shorter and thicker than control samples (Figure 2B). Al^{3+} also caused an aggregation of actin filaments, particularly the shorter strands. Lower concentrations of Al^{3+} caused negligible differences in F-actin

Figure 2. Measurements of the viscosity and organization of rabbit muscle F-actin in the absence and presence of aluminum. ODM measurements of actin in the presence of aluminum at the following concentrations: 0 (gray bars), 50 μM (dark bars), 100 μM (white bars), and 200 μM (light gray bars) (A). Confocal fluorescence images of F-actin (90 $\mu\text{g/ml}$) solutions (from left to right) in the presence of 50, 100, and 200 μM aluminum are shown over the corresponding viscosity measurement. (B).

A



B



solution structures.

Non-muscle actin isolated from human platelets and plant actin isolated from maize pollen were also examined in the presence of aluminum. As seen with muscle actin, Al^{3+} at higher concentrations dramatically decreased the viscosity of non-muscle actin (Figure 3). Addition of 200 μM aluminum shortened non-muscle actin filaments and induced aggregation (Figure 3). Less aggregation of fragments is seen with 100 μM Al^{3+} .

Plant actin exhibits a similar aluminum ion concentration-dependent effect as observed with muscle and non-muscle actins. Addition of 200 μM Al^{3+} lowers solution viscosity to levels approaching baseline (Figure 4). Confocal fluorescence images of plant actin filaments in the presence of 200 μM AlCl_3 show short, aggregated filaments, much like those of muscle and non-muscle actin (Figure 4). These data demonstrate that F-actin from three very different cell types is dramatically altered in a similar fashion following the addition of aluminum.

Al^{3+} Effect is Ion Specific. Alterations in F-actin structure have been investigated for several di- and trivalent cations with atomic radii or charge similar to that of aluminum, at concentration ranges two orders of magnitude higher than were employed in these studies (Barden and Dos Remedios, 1978; Dos Remedios and Barden, 1977). To examine the ion specificity of cation-induced cytoskeletal alterations, the effects of Be^{2+} and La^{3+} on rabbit muscle F-actin were compared to the perturbations induced by Al^{3+} . Whereas 200 μM Al^{3+} substantially decreases the relative viscosity of F-actin, at the same concentration La^{3+} shows no discernible effect, and Be^{2+} may actually cause a slight increase in relative viscosity (Figure 5A). The data clearly show that neither beryllium

Figure 3. The effect of aluminum on the viscosity and organization of human platelet actin. Aluminum was added to solutions of human platelet F-actin (120 $\mu\text{g/ml}$). Confocal fluorescence images of representative F-actin solutions of each sample are shown over the corresponding viscosity measurement.

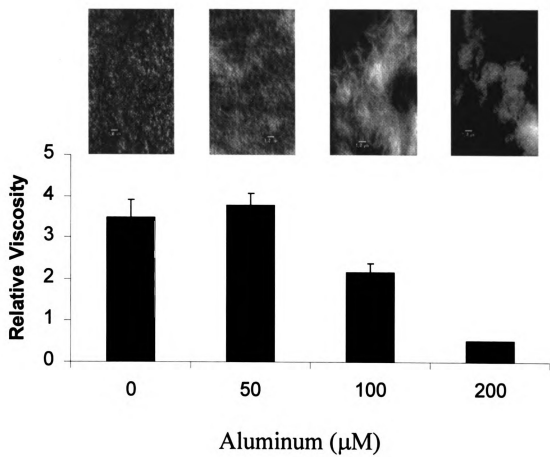


Figure 4. The effect of aluminum on the viscosity and organization of maize pollen actin. Aluminum was added to maize pollen F-actin (240 $\mu\text{g/ml}$) solutions and the samples were then evaluated with ODM. Confocal fluorescence images of each of the maize pollen F-actin solutions are presented in the inset.

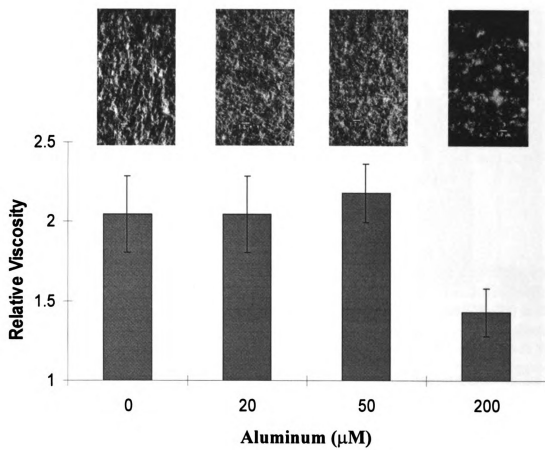
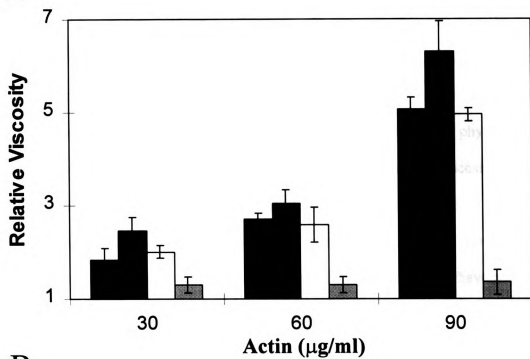
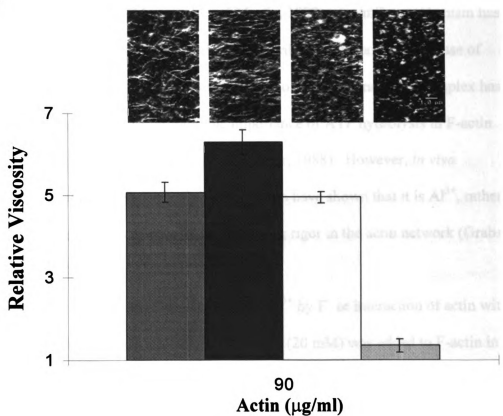


Figure 5. The specificity of aluminum in promoting changes in F-actin networks. ODM measurements of rabbit muscle F-actin (dark gray bars) in the presence of 200 μM aluminum (black bars), beryllium (white bars), and lanthanum (gray bars), respectively (A). Confocal fluorescence images of actin solutions (90 $\mu\text{g}/\text{ml}$) containing each of the ions are shown above the corresponding viscosity measurement. Each metal was utilized at a concentration of 200 μM .

A



B



nor lanthanum can duplicate the effects of aluminum on F-actin.

Rabbit muscle F-actin solutions containing Be^{2+} , La^{3+} , and Al^{3+} were also compared by confocal fluorescence microscopy. As similarly observed from the measurements obtained for relative viscosity, F-actin treated with Be^{2+} or La^{3+} appears much like control actin (Figure 5B). Actin filaments treated with Al^{3+} aggregate and are shorter and thicker than control. These images correspond well with the physical data. Aluminum visibly alters F-actin structure and organization as well as viscosity measurements, whereas beryllium and lanthanum affect neither.

Reversal of Al^{3+} effect by NaF. Fluoride ions bind tightly to Al^{3+} , forming multiple species denoted by AlF_x (Macdonald and Martin, 1988), which have been demonstrated to activate G-proteins (Hepler and Gilman, 1992). AlF_x has been suggested to be a structural analog of PO_4^{3-} , coupling with ADP to mimic $\text{ADP}\cdot\text{P}_i$, the transition state for ATP hydrolysis (Macdonald and Martin, 1988). A similar mechanism has been proposed for G-protein activation with GDP and aluminum fluoride. The use of aluminum fluoride as a cofactor in the formation of a transitional state complex has also been a method employed for probing the importance of ATP hydrolysis in F-actin stability (Allen, et al., 1996; Combeau and Carrier, 1988). However, *in vivo* measurements of actin tension in living plant cells have shown that it is Al^{3+} , rather than the AlF_x complex, that is responsible for inducing rigor in the actin network (Grabski and Schindler, 1995).

To determine if either sequestration of Al^{3+} by F^- or interaction of actin with AlF_x could alter F-actin solution structure, excess NaF (20 mM) was added to F-actin in the presence of aluminum. The excess fluoride reversed the decrease of viscosity of rabbit

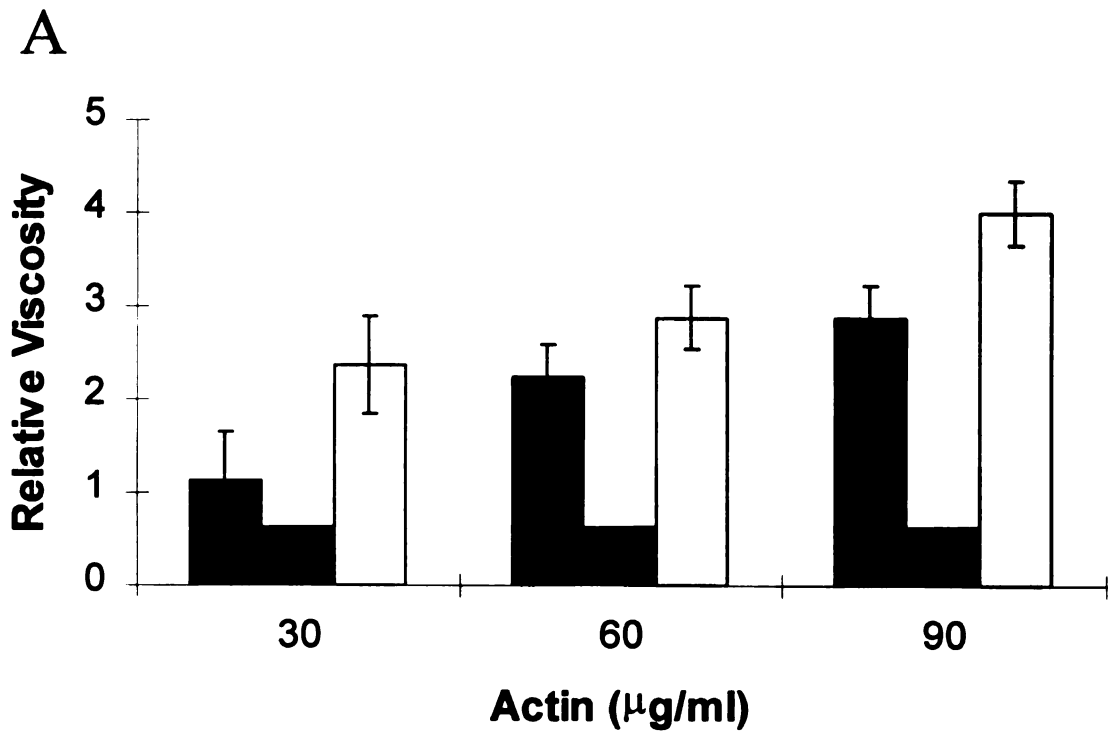
muscle F-actin previously observed following the addition of aluminum (Figure 6A). Sodium fluoride in the absence of aluminum, however, had no noticeable effect on F-actin solutions (data not shown).

Confocal fluorescence microscopy demonstrates that the reversal of the aluminum induced viscosity by sodium fluoride correlates with a reversal in F-actin organization to a structure resembling that of control. Whereas Al^{3+} -treated F-actin is much shorter than the untreated counterpart and is found in large aggregates (Figure 2B), addition of NaF restores filaments to typical lengths and inhibits aggregation (Figure 6B).

Aluminum and ATP. The concentration at which Al^{3+} has its maximum effect on F-actin viscosity (200 μM) matches that of ATP in the assay solution. The literature suggests that Al^{3+} can bind ATP, displacing Mg^{2+} and slowing ATP hydrolysis (Macdonald and Martin, 1988). Though the role of ATP hydrolysis in actin polymerization and stability is still uncertain, such activity could conceivably explain the effects observed with 200 μM aluminum. To test this hypothesis, aluminum-treated actin samples were coincubated with a two-fold excess of ATP. If aluminum were directly inhibiting ATP hydrolysis, then addition of excess ATP should result in an increase in the relative viscosity, perhaps to values approaching those observed for 100 μM AlCl_3 . This was not observed, since the addition of excess ATP had little effect on the viscosity measured for rabbit muscle F-actin (Figure 7). This, in conjunction with evidence presented later in this chapter, provides evidence that the Al^{3+} effect does not result from competition between Al^{3+} and Mg^{2+} for binding sites on ATP.

Although of considerable interest, the *in vitro* results reported above for F-actin interactions with aluminum did not demonstrate the same concentration dependence for

Figure 6. The reversal of the aluminum effect by incubation with NaF. ODM measurements of rabbit muscle F-actin in the presence of 200 μM aluminum or 200 μM aluminum with 20 mM NaF (A). Confocal fluorescence images of F-actin (90 $\mu\text{g}/\text{ml}$) coincubated with the above mentioned ions.



Al	-	+	+		-	+	+		-	+	+
NaF	-	-	+		-	-	+		-	-	+

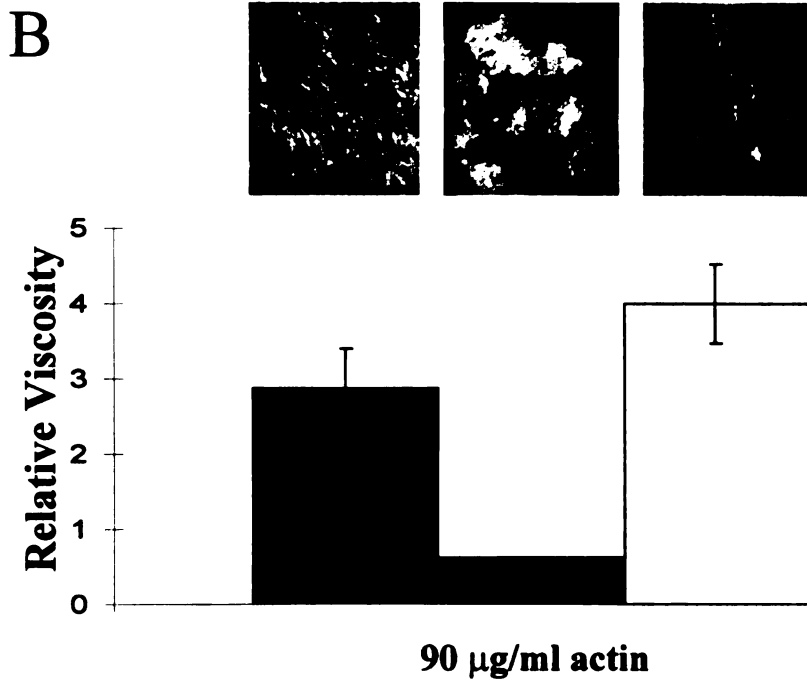
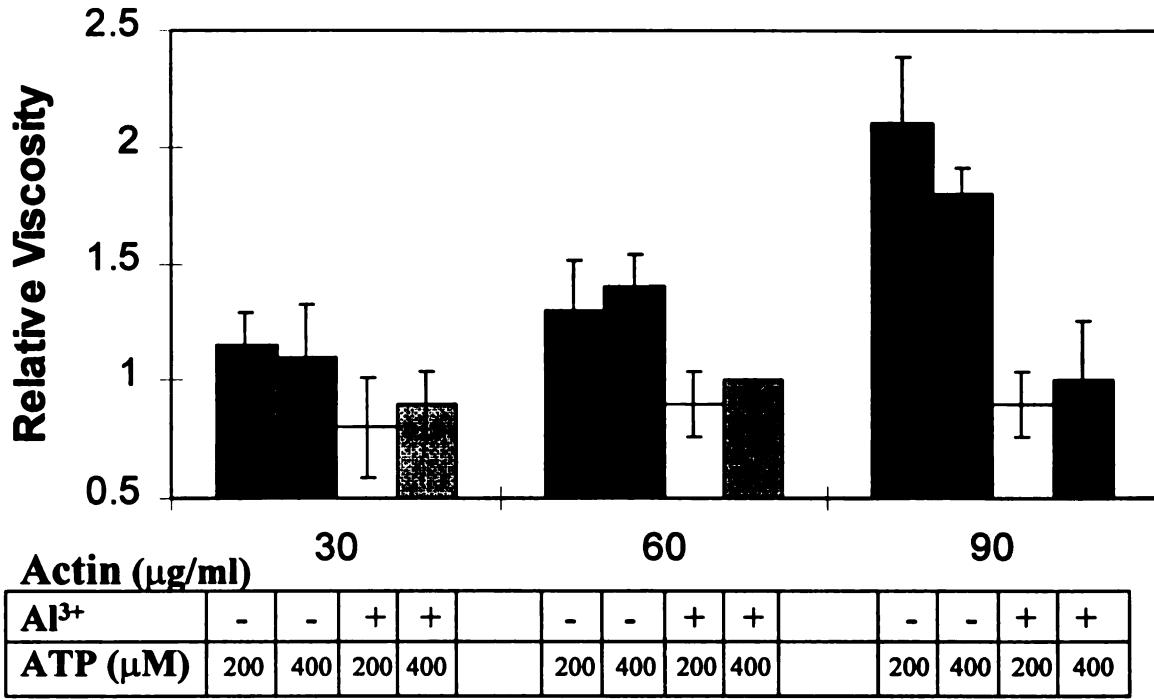


Figure 7. ODM measurements of F-actin solutions in the presence of excess ATP. Rabbit muscle F-actin was polymerized with 200 μM ATP or 400 μM ATP in the absence or presence of 200 μM aluminum at pH 5.8



aluminum activity as was previously reported for tension measurements in live soybean root cells (Grabski and Schindler, 1995). This suggested the possibility that other factors were involved in living cells as targets or mediators of the aluminum activity on actin networks. To examine this more critically, a number of purified actin binding proteins were incorporated into the model system and the effect of aluminum was examined within this more complex reconstituted solution.

The actin-binding protein myosin. Though moderate concentrations of Al^{3+} clearly affect F-actin solution structure, analysis of the data shows that this activity is not adequate to explain the *in vivo* results. Since cellular actin and actin filaments have been shown to interact with a diverse array of other cellular proteins which can bind, bundle, and cross-link the actin filaments (Pollard and Cooper, 1986; Matsudaira, 1991), an accurate *in vitro* model probably requires the addition of one or more of these components. Though animal cells may contain dozens of different actin bundlers and cross-linkers, at present the number or type of such proteins present in plant cells is unknown. To date, only profilin, which interacts with monomeric G-actin, has been well characterized and isolated in reasonable biochemical amounts (Valenta, et al., 1993; Giehl, et al., 1994). Genetic and immunological evidence has also been presented for myosin, a molecular motor (Knight and Kendrick-Jones, 1993; Kinkema and Schiefelbein, 1994); however, isolation of a *bona fide* plant myosin has yet to be demonstrated.

Myosin--A Potential Tension Regulator within the Actin Network

Myosin II is a molecular motor which binds to actin. The tails of myosin monomers interact to form a dimer with two heads which can bind different actin

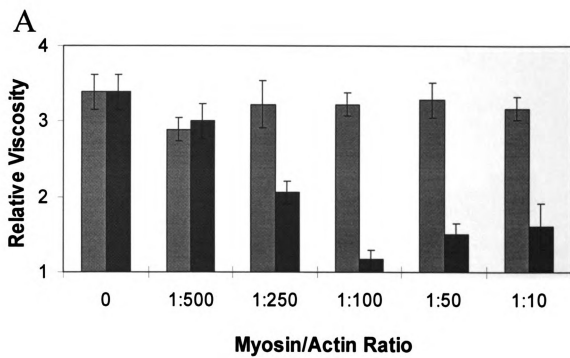
filaments simultaneously. High concentrations of potassium promote myosin filament formation through tail/tail interactions. In this way myosin can act as a cross-linker of actin filaments *in vivo* and *in vitro*.

Addition of low concentrations (1:10 myosin/actin) of bovine muscle myosin II to rabbit muscle F-actin lowered the relative viscosity of the solutions (Figure 8A, black bars). A protein with no reported actin-bundling activity (β -galactosidase) had no significant effect at any concentration (Figure 8A, gray bars).

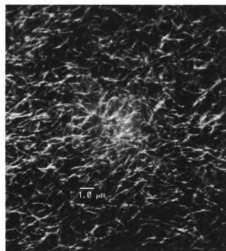
Confocal fluorescence microscopy of myosin/actin solutions revealed localized regions of actin aggregation within a matrix of F-actin filaments (Figure 8B). Aggregates of actin filaments stained with such high intensity that images had to be acquired at reset threshold values. Figures 8B and 8C show neighboring regions on the same microscope slide (1:10 myosin/actin); however, the images have been acquired using different laser intensities (high vs. low) and in different focal planes. All subsequent images of myosin/actin and filamin/actin have been optimized in such a way as to highlight regions of highest staining intensity. It should be noted, however, that though the filament matrix may not be visible as a result of adjusting the sensitivity to detect the fluorescence observed within the aggregates, actin filaments are present throughout all images.

Addition of aluminum to a solution of myosin/actin. Concentrations of aluminum (200 μ M) observed to break down the actin network were also found to disrupt myosin/actin complexes, lowering relative viscosities to near baseline values (data not shown). Following the addition of 20 μ M AlCl_3 , however, relative viscosities increased nearly three-fold for solutions with high myosin/actin ratios (Figure 9A, black bars). Aluminum-induced changes in actin-myosin interaction were not as dramatic when

Figure 8. ODM measurements of solutions of rabbit muscle F-actin in the presence of myosin. ODM rabbit muscle F-actin incubated with bovine muscle myosin II (black bars) or β -galactosidase (gray bars) (A). Confocal fluorescence images of myosin/actin solutions. B and C are images of the same slide at different focal planes. The laser intensity in panel C is significantly less than observed in panel B.



B



C

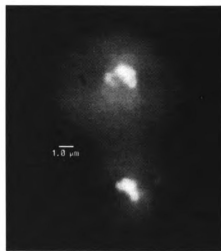
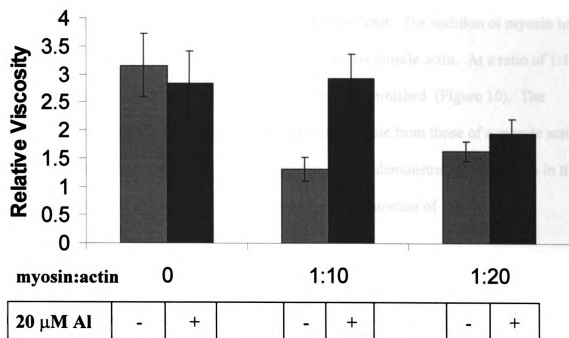
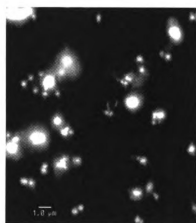


Figure 9. Effect of aluminum on solutions of rabbit muscle F-actin/bovine muscle myosin II. ODM measurements of solutions of myosin/actin in the absence or presence of aluminum (20 μM) (A). Confocal fluorescence images of myosin/actin (1:10 myosin/actin) in the absence or presence of aluminum (20 μM) (B).

A

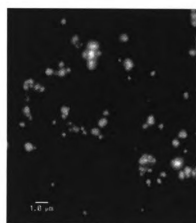


B



Myosin

C



+ Al

viewed with a confocal microscope. Myosin/actin bundles appear to be more dispersed in the presence of aluminum (Figure 9B and 9C); aggregates appear to be smaller, though more plentiful, under these conditions.

Non-muscle actin with myosin. Bovine muscle myosin II was similarly added to human platelet actin and allowed to equilibrate for one hour. The addition of myosin had virtually the same effect on non-muscle actin as it did on muscle actin. At a ratio of 1:10 myosin/actin, the viscosity of the solution was greatly diminished (Figure 10). The confocal fluorescence images are virtually indistinguishable from those of a muscle actin solution containing myosin (Figure 10). The data clearly demonstrate that changes in the viscosity of F-actin solutions are dependent on the concentration of myosin that is coincubated with the actin.

Upon addition of AlCl_3 (20 μM) to solutions of non-muscle actin containing myosin, an approximate 3-fold increase in viscosity was observed which was similar to that shown with muscle actin (Figure 11). Images of these samples reveal that the addition of aluminum seems to result in a more ordered distribution of myosin/actin aggregates throughout the field of view (Figure 11). In the aluminum treated sample, images were taken in two different focal planes at the same X and Y coordinates in order to illustrate the extent of interaction between bundles of actin filaments.

Plant actin with myosin. Bovine muscle myosin II was also incubated with F-actin from maize pollen. As shown with both muscle and non-muscle actin, a ratio of 1:10 myosin/actin causes the greatest alteration in solution viscosity (Figure 12). Lower amounts of myosin have increasingly diminishing effects on the solutions. Confocal

Figure 10. ODM measurements of solutions of myosin/non-muscle F-actin. ODM measurements of human platelet actin (120 $\mu\text{g/ml}$) in the presence of bovine muscle myosin II. Confocal fluorescence microscopy images of the myosin/actin solutions at the indicated ratios.

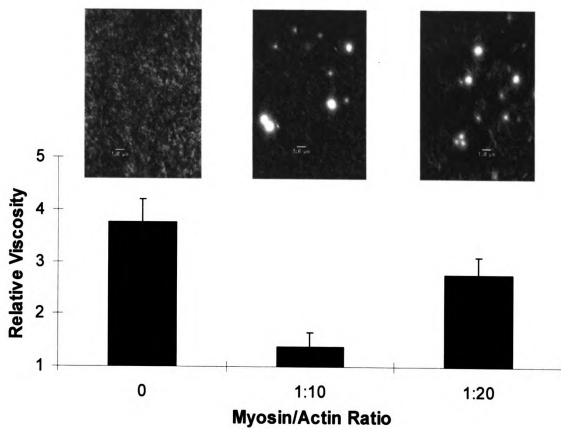


Figure 11. Effect of aluminum on solutions of myosin/non-muscle actin. ODM measurements of 120 $\mu\text{g/ml}$ actin/myosin in the absence (gray bars) and presence (black bars) of 20 μM aluminum. The two images at right are obtained at different focal planes from the same region.

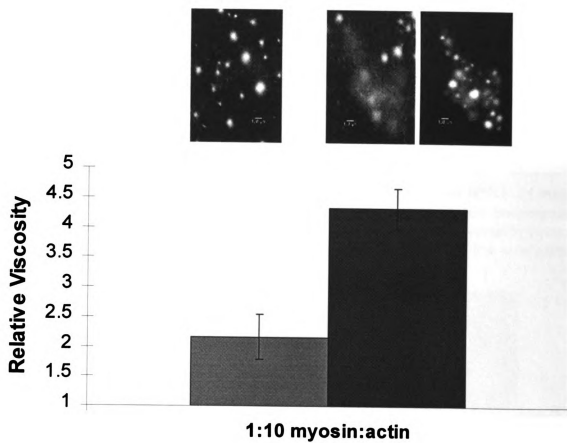
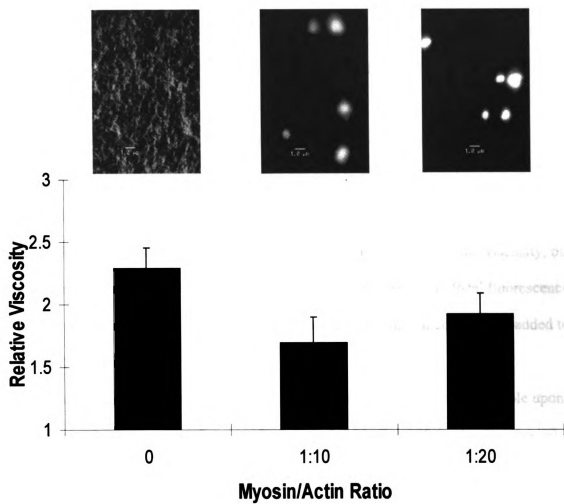


Figure 12. ODM measurements of myosin/maize pollen actin solutions. ODM measurements were performed on solutions of maize pollen actin (240 $\mu\text{g/ml}$) in the presence of bovine muscle myosin II. Confocal fluorescence micrographs of myosin/actin at the indicated ratios are paired with the viscosity measured for the sample.



fluorescence microscopy reveals the now-familiar bundles of actin and myosin (Figure 12).

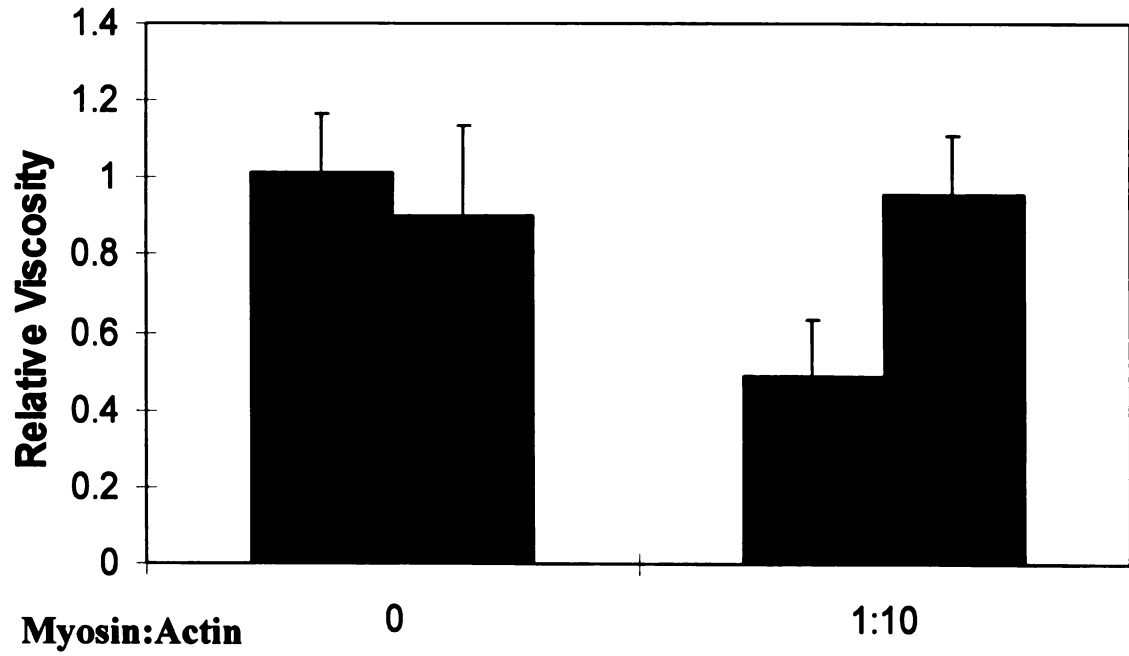
Low concentrations of aluminum (20 μM) have the same qualitative effect on the viscosity of myosin/actin complexes as they did with muscle and non-muscle actin. Addition of aluminum increases the relative viscosity by more than two-fold (Figure 13). However, little change in solution structure can be seen upon incubation with AlCl_3 (data not shown).

Ion specificity of aluminum effect. The aluminum-induced changes in the organization of myosin/actin complexes and solution viscosity are ion-specific. Addition of beryllium (20 μM), copper (20 μM), or zinc (20 μM) have no effect on viscosity of the samples (Figure 14). Twenty micromolar lanthanum may slightly increase viscosity, but these changes are considerably less than observed for aluminum. Confocal fluorescence microscopy showed no differences between control and any ion other than Al^{3+} added to samples (data not shown).

The aluminum-induced rigor within the plant actin network was reversible upon the addition of excess sodium fluoride (Grabski and Schindler, 1995). As was previously observed with F-actin solutions, addition of 2 mM NaF to myosin/actin pre-incubated with 20 μM AlCl_3 completely reversed the *in vitro* effects of Al^{3+} (Figure 15). Slides of myosin/actin with NaF and AlCl_3 look virtually indistinguishable from those which had neither NaF nor AlCl_3 , showing reversal of the aluminum effect (data not shown). These results and concentrations are consistent with those seen *in vivo*.

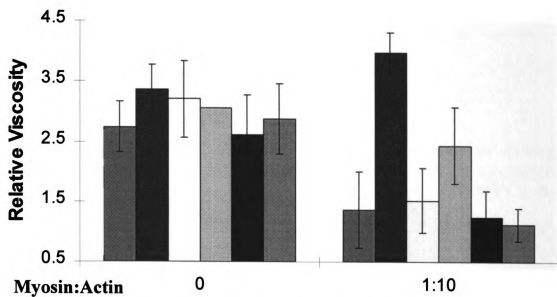
Heating of myosin. Heating myosin at 47.5° C for two minutes has been shown to drastically reduce its motility and ATPase activity *in vivo* (Kohn and Shimmen, 1988).

Figure 13. Effect of aluminum on myosin/maize pollen actin solutions. ODM measurements of bovine muscle myosin II/maize pollen actin in the absence and presence of 20 μ M aluminum.



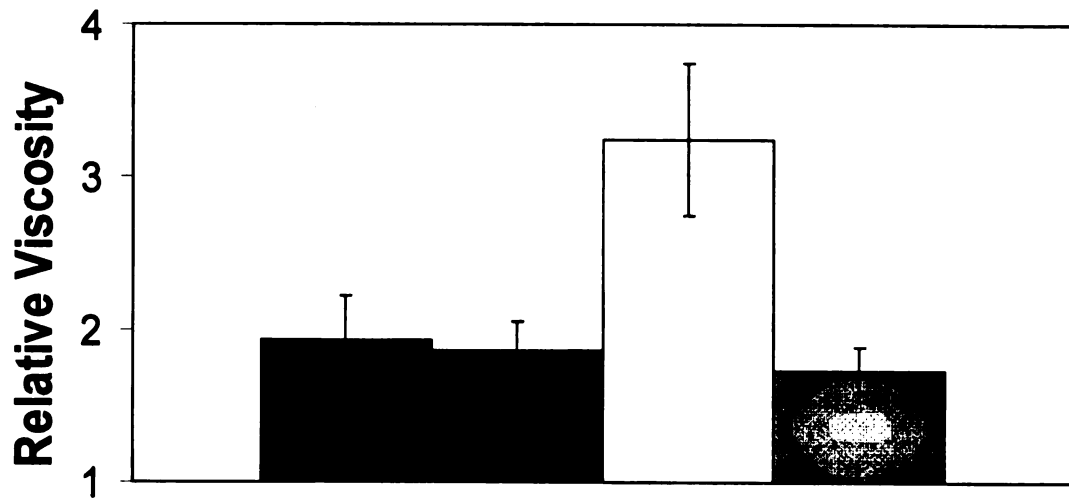
Al ³⁺		-	+		-	+
------------------	--	---	---	--	---	---

Figure 14. The effect of aluminum on myosin/actin complexes is specific. ODM measurements of bovine muscle myosin II/rabbit muscle F-actin solutions in the presence of 20 μM aluminum , beryllium, lanthanum, copper (II), and zinc.



Al³⁺	-	+	-	-	-	-	-	-	+	-	-	-	-
Be²⁺	-	-	+	-	-	-	-	-	-	+	-	-	-
La³⁺	-	-	-	+	-	-	-	-	-	-	+	-	-
Cu²⁺	-	-	-	-	+	-	-	-	-	-	-	+	-
Zn²⁺	-	-	-	-	-	+	-	-	-	-	-	-	+

Figure 15. Reversal of aluminum-induced viscosity change by fluoride. ODM measurements of 1:10 myosin II/muscle actin with or without aluminum (20 μ M) in buffer \pm 2 mM NaF.



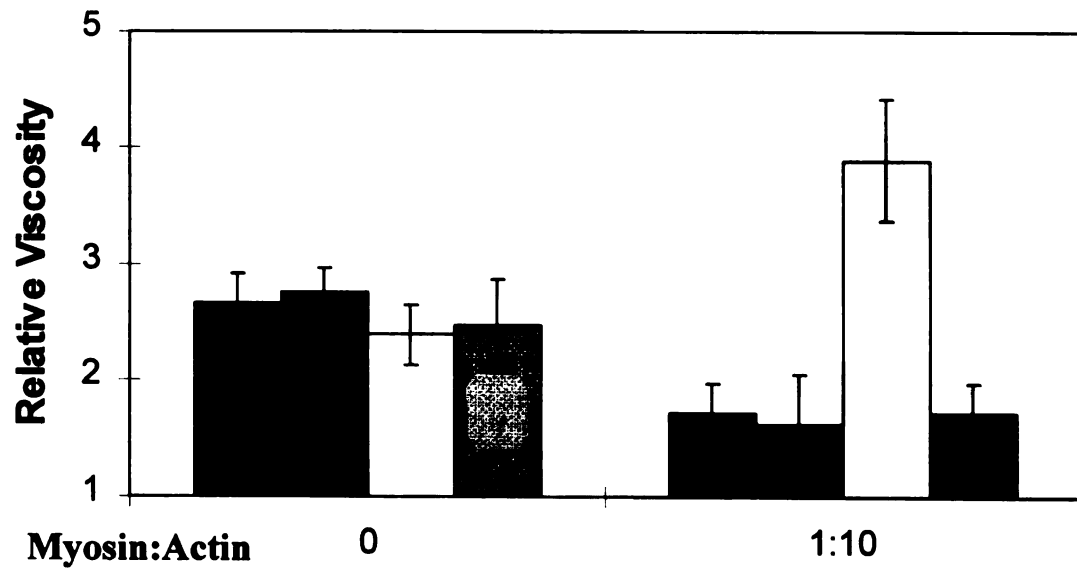
Al³⁺	-	-	-	-
NaF	-	+	-	+

But heating the samples at 47.5° C for 2 minutes did not affect the drop in viscosity of rabbit muscle F-actin following the addition of bovine muscle myosin II (Figure 16). However, heat treatment did abolish the aluminum-induced increase in relative viscosity. This suggests that heat may be altering the structure of myosin or myosin/actin complexes, inhibiting their interactions with aluminum. As shown later, heating also significantly diminished the ATPase activity of myosin (Figure 19).

These experiments did not rule out the possibility that aluminum was only affecting viscosity changes caused by myosin filament formation. Attempts to use ODM to analyze solutions containing myosin in the absence of actin were unsuccessful because the polystyrene microspheres used in ODM adhered to the surfaces of the microscope slides. To pursue these measurements, the samples were examined with a Cannon-Manning semi-micro-capillary viscometer (Cannon Instrument Co., State College, PA). Aluminum does not cause measurable differences in the viscosity of solutions containing bovine muscle myosin II (Figure 17), indicating that the observed aluminum effect requires the presence of both actin and myosin. Whether this is a property unique to myosin/actin interactions (perhaps through myosin ATPase activity), or it is a general phenomenon observed with any actin-bundling protein, is a topic to be addressed later in this chapter.

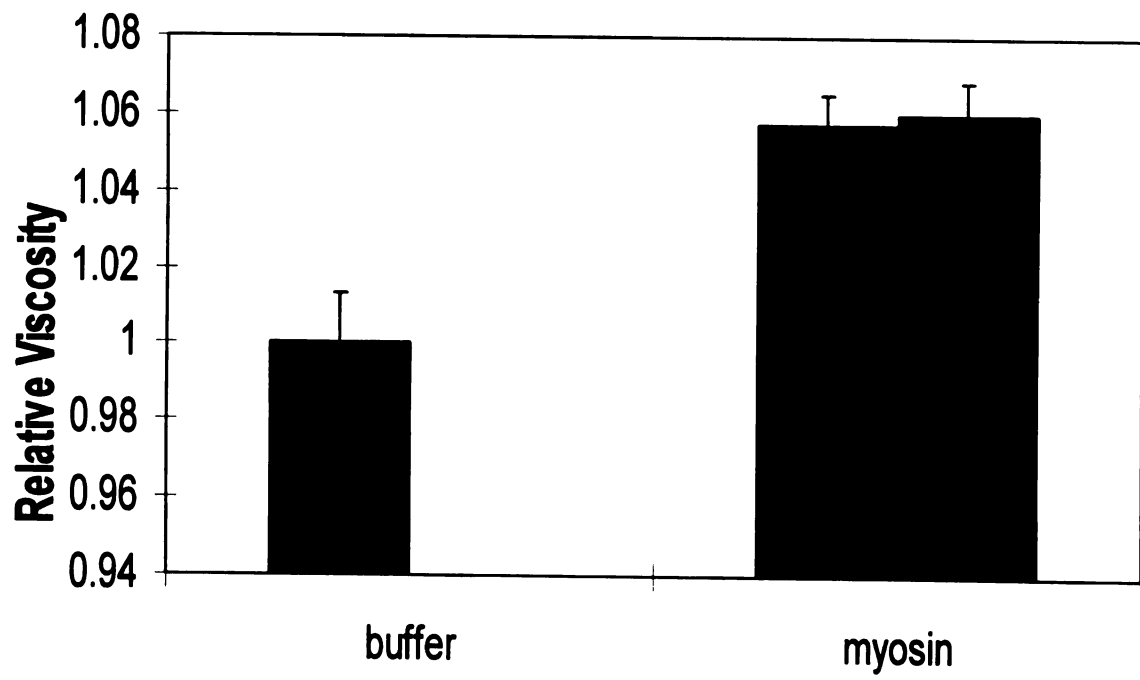
Intact actin network is necessary for the Al³⁺ effect. Equilibrated bovine muscle myosin II/rabbit muscle actin gels were disrupted with cytochalasin D or latrunculin B (a toxin isolated from Red Sea sponge which reversibly disrupts the organization of microfilaments (Coué, et al., 1987)). Addition of either reagent to disrupt filaments prevents the action of aluminum, showing that an intact F-actin network is necessary for

Figure 16. Heat treatment inhibits the effect of aluminum on the viscosity and organization of solutions of myosin/actin. ODM measurements of bovine muscle myosin II/rabbit muscle F-actin with or without heating at 47.5° C for 2 minutes. Buffer \pm 20 μ M aluminum was added.



heat	-	+	-	+		-	+	-	+
Al³⁺	-	-	+	+		-	-	+	+

Figure 17. Capillary viscometry of bovine muscle myosin II. Semi-micro capillary viscometry of myosin ($0.267 \mu\text{M}$) in the absence (gray bars) and presence (black bars) of $20 \mu\text{M}$ aluminum.



aluminum to have any effect on solution viscosity (Figure 18). Without an intact actin filament network, viscosity values remain near baseline.

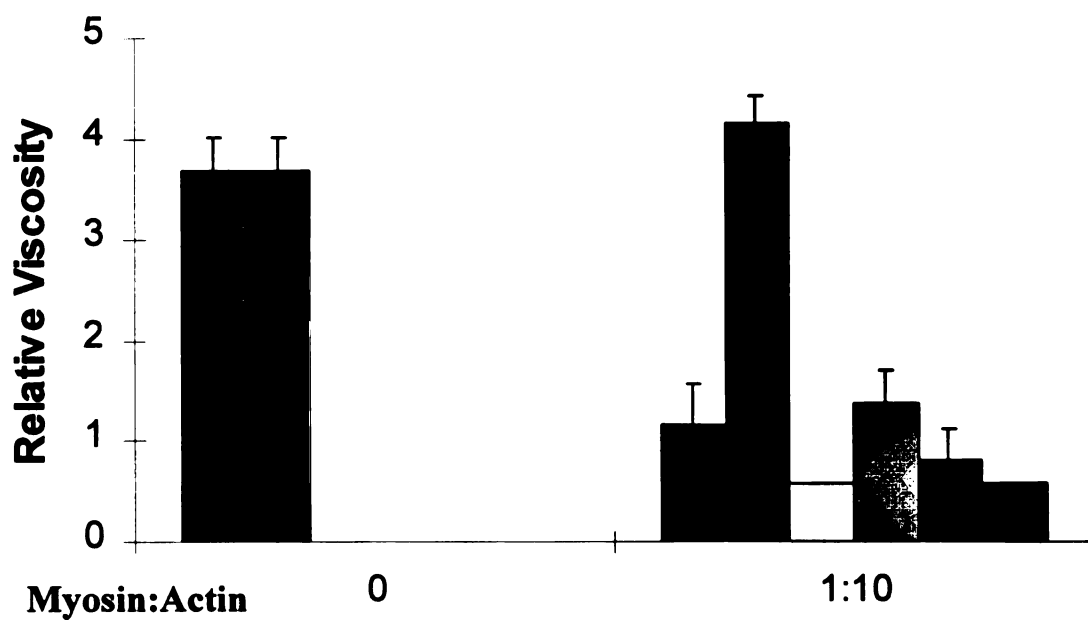
ATPase assays. As shown in the previous section, low concentrations of aluminum (20 μM) can significantly increase the viscosity of solutions containing myosin/actin complexes; however, these same concentrations of aluminum have no effect on solutions of actin without an actin bundling protein such as myosin. One possible mechanism of enhanced aluminum activity in the presence of myosin is through alteration of the myosin ATPase activity, either by stabilizing ATP against hydrolysis or by a direct interaction with myosin itself. To test this hypothesis, we used a luciferase-luciferin ATPase assay to examine the ATPase activity of myosin in the absence and presence of aluminum.

Addition of aluminum to assay solutions at pH 5.8 had no effect on ATPase activity (Figure 19). Myosin ATPase activities were calculated by comparing the amount of ATP remaining after 30' of reaction to the amount of ATP present at the start of each reaction. All values were normalized against the activity of actin-activated myosin ATPase activity. Addition of 20 μM Al^{3+} had little effect on the amount of ATP hydrolyzed by myosin in 30'. Heated myosin, whose activity was diminished by almost fifty percent, served as a positive control for decreases in ATPase activity. These data demonstrate that the effect of 20 μM aluminum on actin networks containing myosin is independent of the myosin ATPase activity.

The actin-bundling protein filamin.

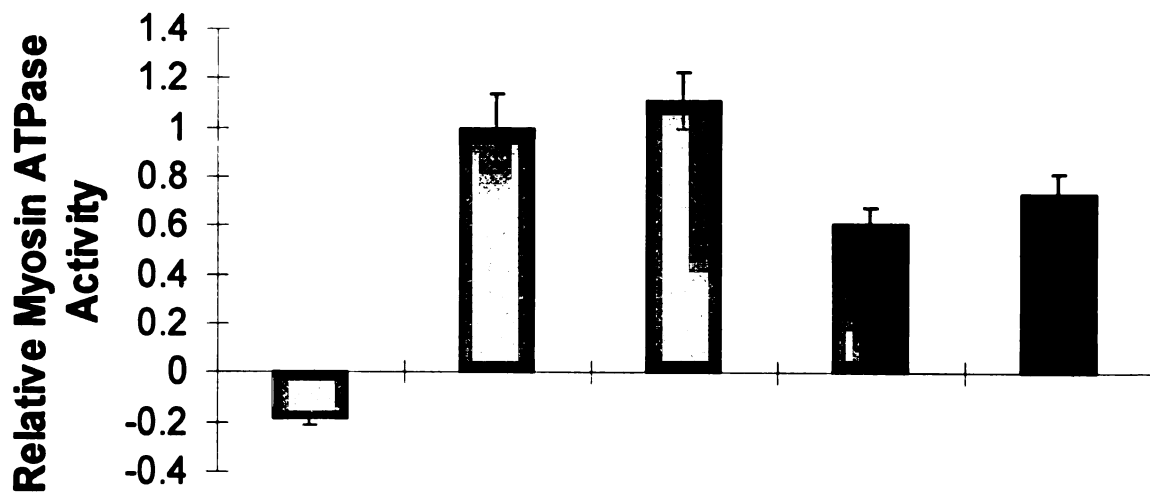
The results described above for myosin suggest that the binding of myosin to actin filaments and the subsequent bundling by myosin, rather than its ATPase activity,

Figure 18. The effect of cytochalasin D and latrunculin on aluminum-induced changes in solutions of myosin/actin. ODM measurements of bovine muscle myosin II/rabbit muscle F-actin in buffer, cytochalasin D (2 μM), or latrunculin B (2 μM). ODM measurements were made in the presence or absence of 20 μM aluminum.



Al^{3+}	-	+	-	+	-	+
cytochalasin D	-	-	+	+	-	-
latrunculin B	-	-	-	-	+	+

Figure 19. Assays of myosin ATPase activity. Actin-activated myosin ATPase activity is demonstrated in the absence and presence of aluminum \pm heat treatment of myosin.



Myosin + 0.2 mg/ml actin	+	+	+	+
Al³⁺	-	+	-	+
heat	-	-	+	+

are responsible for increasing the sensitivity of the actin network to aluminum. To further pursue this line of reasoning, filamin was employed in the model system as an independent actin cross-linking protein. It was proposed that if the bundling of actin were necessary and sufficient to enhance the activity of aluminum within the actin network, then filamin, an actin cross-linking protein that is active as a homodimer with no ATPase activity (Janson, et al., 1991), should induce the same enhanced sensitivity to aluminum.

Human platelet filamin was added to rabbit muscle actin and the solutions were allowed to equilibrate for one hour at room temperature. Amounts of filamin were varied against a constant actin concentration. As the filamin/actin ratios increased, the relative viscosity also increased (Fig 20, black bars). In contrast, β -galactosidase, a protein of similar molecular weight which has not been demonstrated to bind actin, exhibited little effect on the ability of an actin solution to impede the movement of optically trapped polystyrene beads (Figure 20, gray bars). Confocal fluorescence images clearly show bundles of actin filaments upon addition of filamin (Figure 20).

Aluminum and Filamin/Actin Complexes

Addition of low concentrations of aluminum (20 μ M) at pH 5.8 to filamin/actin networks caused further increases in relative viscosity over a wide range of filamin/actin ratios (Figure 21A). For 1:50 filamin/actin, there was a three-fold enhancement in viscosity following the addition of Al^{3+} . Visualization of filamin/actin networks in the absence and presence of Al^{3+} shows dramatic differences between the two, especially at 1:50 filamin actin (Figure 21B). Aluminum caused a noticeable clouding of the field of view, hinting of a large interlinked network of bundles of filamin/actin filaments.

Figure 20. ODM measurements of solutions of filamin/actin. ODM measurements of rabbit muscle actin (120 $\mu\text{g/ml}$) coincubated with chicken gizzard filamin (black bars) or recombinant β -galactosidase (gray bars). Confocal fluorescence images of the filamin/actin solutions are shown above the viscosity measurement for a given sample.

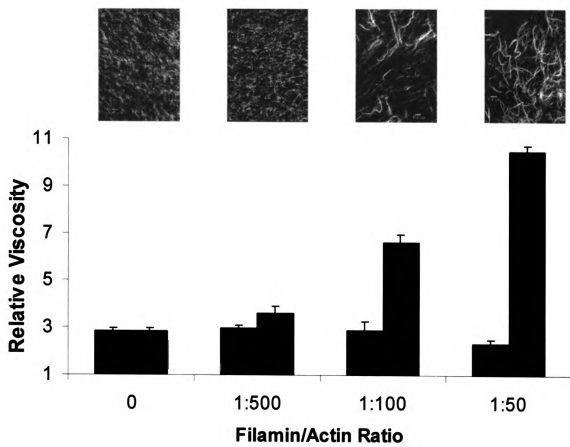
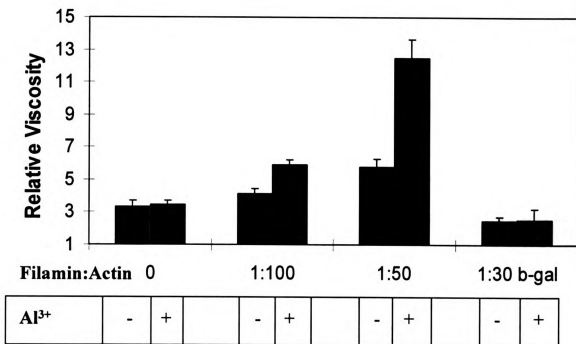
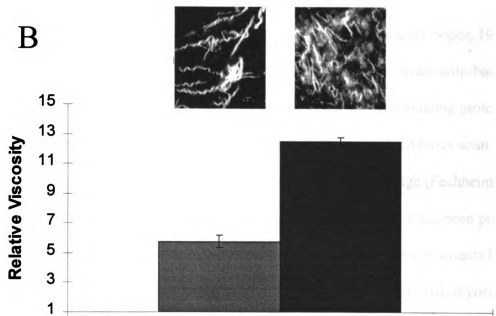


Figure 21. Effect of aluminum on solutions of filamin/actin. ODM measurements on solutions of chicken gizzard filamin/actin in the absence or presence of 20 μ M aluminum (A). Confocal fluorescence images of filamin/actin (1:50) in the absence or presence of aluminum (B).

A



B



DISCUSSION

The ODM measurements described in Chapter Two demonstrated that aluminum could alter the viscosity of solutions of actin filaments derived from a variety of sources. The results demonstrated that *high* concentrations of aluminum (200 μM) resulted in a *decrease* in the viscosity of all the actin samples. These measurements, however, contrasted with the *in vivo* measurements in which aluminum was found to *increase* the tension within the actin network at *low* concentrations of aluminum (20 μM). The concentration differences for aluminum activity observed between the *in vivo* and *in vitro* systems and the apparent opposite physical response of actin to aluminum observed between the two systems suggested that the reconstituted model system might require additional components to be more representative of the response of actin filaments to aluminum in living cells.

In the cell, a number of different proteins interact with actin filaments, linking them to each other, to other proteins, and to membranes (Pollard and Cooper, 1986). Alteration of any of these interactions could have a drastic effect on all actin-based functions within the cell. A review of the plant literature for actin-binding proteins reveals the rigorous characterization of only profilin, a protein which binds actin monomers and may sequester them or facilitate ADP/ATP exchange (Fechheimer and Zigmond, 1993). A more limited identification and characterization has been provided for a plant type myosin. To determine whether cross-linking of actin filaments by actin binding proteins was important for the aluminum effect observed in cells, myosin and filamin were added in separate experiments to solutions of actin from diverse sources in the absence and presence of aluminum.

In the reconstituted system, myosin lowered solution viscosities noticeably. This could be easily interpreted in the context of the micrographs—F-actin was sequestered in regions of high density, but the extent of actin polymerization did not look altered. Addition of low concentrations of aluminum (20 μM) provided a dramatic increase in viscosity which was consistent with the *in vivo* data. Of particular relevance was the observation that these changes were also observed with both non-muscle and maize pollen actin; actins from three different cell types gave the same result, suggesting a common mechanism.

Observations by Washsstock et al. (1994) help suggest a model which reconciles the *in vitro* and *in vivo* results. Washsstock and colleagues (1993) had earlier reported that the affinity for actin of a crosslinker determines the structure of actin filament gels. Tightly crosslinked bundles of actin filaments which cannot easily slide past each other will resist deformation against an applied force (Washsstock et al., 1994). Likewise, changes in bundling or crosslinking in a filament network will alter solution viscosity (Hou, et al., 1990). A mechanism in which aluminum modified actin filament crosslinking could account for both the *in vitro* and *in vivo* effects.

An *in vitro* model is valuable only to the extent that it mimics the *in vivo* phenomena. Aluminum concentrations necessary to induce changes in the actin system reconstituted with myosin or filamin correspond well with the *in vivo* results. Further, there is a similar ion specificity observed for the induction of structural and physical changes within the actin network (Grabski and Schindler, 1995). The aluminum effect can be reversed upon incubation with F^- , causing formation of AlF_x , or by heating solutions at 47.5° for as little as two minutes. All of these support our proposal for the

necessity of a cross-linked actin network in the model system to enhance the efficacy of aluminum in altering the chemical and physical properties of the actin network to that observed in whole cells .

But how might aluminum be acting? In plant cells, the most likely candidate for an actin bundler is myosin. Aluminum may be affecting one or both of the *in vivo* activities of myosin. The low Al^{3+} concentrations used in this study do nothing to alter the ATPase activity of myosin. The other *in vivo* activity of myosin that Al^{3+} may be targeting is its actin cross-linking ability resulting from myosin tail-tail interactions. Experiments with filamin, an actin cross-linking protein with no ATPase activity, confirm this, for addition of aluminum also results in sizeable increases in solution viscosities of filamin/actin samples reminiscent of those seen with actomyosin.

Actin filaments can have a net negative charge of up to (-)14/subunit (Tang and Janmey, 1996). Aluminum may bind in such a way that it bridges the negative charges of adjacent actin filaments. Bundling of filaments through myosin or filamin may facilitate the action of aluminum by bringing many filaments in closer proximity to each other. In a solution of only actin, the effects of aluminum may not be enough on their own to noticeably alter the filamentous structure of actin. However, the strong association between filaments brought about by a bundling protein may be enough to enhance the number of binding sites for aluminum or the efficacy of aluminum to cross-link actin, resulting in enhanced tension within the actin network and an increase in viscosity of the F-actin solution.

As yet unpublished observations from this lab support this hypothesis. Inhibitor studies reveal that calcium regulated protein kinases (calmodulin-like domain protein

kinase and/or a calcium/calmodulin-dependent protein kinase) and phosphatases (calcineurin or calcinerin-type) can affect actin tension within the plant cell cytoskeleton (Grabski, et al., 1998). Interestingly, upon addition of kinase inhibitors, aluminum no longer has much effect on the tension within the actin network, and filament stability is greatly diminished. Since myosin can be activated by phosphorylation (Janson et al., 1991) the inhibitors may affect the conformation of myosin and modify its ability to bind and bundle F-actin. But since kinases and phosphatases either add or remove phosphates from the head group of myosin, alteration in their activity will affect the charge of myosin and presumably affect the interactions of myosin with the actin filaments and the interaction of filaments with each other. If the cation Al^{3+} is bridging negative charges between filaments, changes in charges will greatly affect the bundling activity. These results are consistent with the data presented in this chapter.

Evidence from confocal fluorescence microscopy also supports this interpretation. Images from either myosin/actin (especially non-muscle myosin) or filamin/actin solutions have similar characteristics upon addition of Al^{3+} (20 μ M). Instead of the tight, defined structures of actin aggregation seen before addition of aluminum, a disperse cloud of actin filaments is seen linking aggregates in a complex network. These images support the conclusion that Al^{3+} can cause multiple associations between adjacent filaments and bundles of filaments. Interactions between filaments would raise solution viscosity *in vitro* and dramatically alter filament behavior *in vivo*.

A dynamic actin network is vitally important for its function in cell-division, organelle localization, and transport of raw material throughout the cell. Agents which alter either filament polymerization or filament/filament associations can greatly

compromise the integrity of the cell, leading to serious consequences for the organism (Cooper, 1987). The work detailed herein provides an *in vitro* model for the effects of aluminum on the plant cell actin network. Further work with actin mutants and mutant actin binding proteins in model systems should help to further clarify the mechanism of aluminum as a cytoskeletal toxicant.

REFERENCES

- Allen PG, Laham LE, Way M, Janmey PA (1996) Binding of phosphate, aluminum fluoride, or beryllium fluoride to F-actin inhibits severing by gelsolin. *J Biol Chem* **271**: 4665-70
- Bard F, Franzini-Armstrong C, Ip W (1987) Rigor cross-bridges are double-headed in fast muscle from crayfish. *J Cell Biol* **105**: 2225-34
- Barden JA, Dos Remedios CG (1978) Evidence for the non-filamentous aggregation of actin induced by lanthanide ions. *Biochim Biophys Acta* **537**: 417-27
- Combeau C, Carlier MF (1988) Probing the mechanism of ATP hydrolysis on F-actin using vanadate and the structural analogs of phosphate BeF_3^- and AlF_4^- . *J Biol Chem* **263**: 17429-36
- Cooper JA (1987) Effects of cytochalasins and phalloidin on actin. *J Cell Biol* **105**: 1473-8
- Coué M, Brenner SL, Spector I, Korn ED (1987) Inhibition of actin polymerization by latrunculin A. *FEBS Lett* **213**: 316-8
- Delhaize E, Ryan PR (1992) Aluminum toxicity and tolerance in plants. *Plant Physiol* **107**: 315-21
- Dos Remedios CG, Barden JA (1977) Effects of Gd(III) on G-actin: Inhibition of polymerization of G-actin and activation of myosin ATPase activity by Gd-G-actin. *Biochem Biophys Res Comm* **77**: 1339-46
- Fechheimer M, Zigmond SH (1993) Focusing on unpolymerized actin. *J Cell Biol* **123**: 1-5
- Flaten TP, Alfrey AC, Birchall JD, Savory J, Yokel RA (1996) Status and future concerns of clinical and environmental aluminum toxicology. *J Tox Env Health* **48**: 527-41
- Giehl K, Valenta R, Rothkegel M, Ronsiek M, Mannherz HG, Jockusch BM (1994) Interaction of plant profilin with mammalian actin. *Eur J Biochem* **226**: 681-9
- Grabski S, Arnoys E, Busch BA, Schindler M (1998) Dynamic modification of tension within the actin network in plant cells by calcium regulated kinases and phosphatases. *Plant Physiol* **116**: 279-90

- Grabski S, Schindler M (1995) Aluminum induces rigor within the actin network of soybean cells. *Plant Physiol* **108**: 897-901
- Hepler JR, Gilman AG (1992) G proteins. *TIBS* **17**: 383-7
- Janson LW, Kolega J, Taylor DL (1991) Modulation of contraction by gelation/solution in a reconstituted motile model. *J Cell Biol* **114**: 1005-15
- Kinkema M, Schiefelbein J (1994) A myosin from a higher plant has structural similarities to class V myosins. *J Mol Biol* **239**: 591-7
- Knight AE, Kendrick-Jones J (1993) A myosin-like protein from a higher plant. *J Mol Biol* **231**: 148-54
- Kohno T, Shimmen T (1988) Accelerated sliding of pollen tube organelles along *Characeae* actin bundles regulated by Ca^{2+} . *J Cell Biol* **106**: 1539-43
- Laemmli UK (1970) Cleavage of structural proteins during the assembly of the head of bacteriophage T4. *Nature* **227**: 680-5
- Lowry OH, Rosenburg NJ, Farr AL, Randall RJ (1951) Protein measurement with Folin phenol reagent. *J Biol Chem* **193**: 265-75
- Macdonald TL, Martin RB (1988) Aluminum ion in biological systems. *TIBS* **13**: 15-9
- Matsudaira P (1991) Modular organization of actin crosslinking proteins. *TIBS* **16**: 87-92
- Pardee JD, Spudich JA (1982) Purification of muscle actin. *Meth Cell Biol* **24**: 271-89
- Pollard TD, Cooper JA (1986) Actin and actin-binding proteins. A critical evaluation of mechanisms and functions. *Ann Rev Biochem* **55**: 987-1035
- Sparling DW, Lowe TP (1996) Environmental hazards of aluminum to plants, invertebrates, fish, and wildlife. *Rev Env Con Tox* **145**:1-128
- Tang JX, Janney PA (1996) The polyelectrolyte nature of F-actin and the mechanism of actin bundle formation. *J Biol Chem* **271**: 8556-63
- Valenta R, Ferreira F, Grote M, Swoboda I, Vrtala S, Duchêne M, Deviller P, Meagher RB, McKinney E, Heberle-Bors E, Kraft D, Scheiner O (1993) Identification of profilin as an actin-binding protein in higher plants. *J Biol Chem* **268**: 22777-81
- Wachsstock DH, Schwarz WH, Pollard TD (1994) Cross-linker dynamics determine the mechanical properties of actin gels. *Biophys J* **66**: 801-9

Chapter 4

CONCLUDING STATEMENT

Absorption of aluminum from acidic soils and surface waters can have significant adverse consequences for plant growth and development. Such deleterious effects range from stunted root growth to death. Despite the agricultural importance of the problem and years of intense study, investigations have yielded neither definitive targets nor unambiguous molecular mechanism(s) for aluminum toxicity in plant cells.

This dissertation describes the development of a new assay, Optical Displacement Microviscometry (ODM), to measure the viscosity of actin solutions in a reconstituted model system. The experiments performed with this technique in a reconstituted system were designed to characterize the components and interactions within the actin network and their interactions that are potentially affected by the addition of aluminum. An attractive feature of the ODM technique is that it utilizes a laser optical trap to perform viscosity measurements in microvolumes of solution ($\sim 10 \mu\text{l}$) and only requires minute quantities of precious sample. Confocal fluorescence microscopy was utilized in conjunction with the ODM technique to examine the organization of the actin network. Results obtained from both techniques were employed to correlate the organization of the filament networks within the reconstituted system to the viscosity of the actin solution.

In pure actin solutions, the effects of aluminum were not apparent until after the

addition of high concentrations. However, inclusion of an actin binding protein that cross-links actin filaments, e.g. myosin or filamin, altered the organization of the actin solution in a way that decreased the concentration of aluminum ($20\ \mu\text{M}$) that was required to cause dramatic effects on the measured viscosity. The changes in the viscosity of myosin/actin solutions induced by aluminum were observed regardless of the type of actin (rabbit muscle, human platelet, or maize pollen) examined in the model system. The changes in viscosity observed with aluminum could be seen with confocal fluorescence microscopy as alterations in the organization and interaction of actin filaments. The data obtained using the reconstituted actin systems, the ODM, and confocal fluorescence microscopy provide support for a mechanism of aluminum toxicity in which physiologically relevant concentrations of aluminum can promote/enhance the interaction of actin filaments in the presence of actin crosslinking proteins resulting in abnormal functioning of actin dependent cellular processes.

MICHIGAN STATE UNIV. LIBRARIES



31293017129119